FLOW MEASUREMENT IN TRAPEZOIDAL OPEN CHANNELS WITH PROFILER AND PROPELLER CURRENT METERS

A DISSERTATION

Submitted in partial fulfillment of the requirements for the award of the degree of

MASTER OF TECHNOLOGY

in

ELECTRICAL ENGINEERING

(With Specialization in Measurement and Instrumentation)

By

KASUNDRA SANJAY KUMAR BHAGVANJI

DEPARTMENT OF ELECTRICAL ENGINEERING
INDIAN INSTITUTE OF TECHNOLOGY ROORKEE
ROORKEE - 247 667 (INDIA)
JUNE, 2007

I.D. No.-M.T. 411/2007-GK/HKV-BKG

CANDIDATE'S DECLARATION

I hereby declare that the work that is being presented in this dissertation report entitled **"FLOW MEASUREMENT IN TRAPEZOIDAL OPEN CHANNELS WITH PROFILER AND PROPELLER CURRENT METERS"** submitted in partial fulfillment of the requirements for the award of the degree of **Master of Technology** in **Electrical Engineering** with specialization in **MEASUREMENT AND INSTRUMENTATION**, to the **Department of Electrical Engineering, Indian Institute of Technology, Roorkee**, is an authentic record of my own work carried out, under the guidance of **Dr. H. K. VERMA**, Professor, Department of Electrical Engineering and **Dr. B. K. GANDHI**, Professor, Department of Mechanical and Industrial Engineering.

The matter embodied in this dissertation report has not been submitted by me for the award of any other degree or diploma.

Date: 30/06/07

Place: Roorkee

(KASUNDRA SANJAY KUMAR BHAGVANJI)

This is to certify that the above statement made by the candidate is correct to the best of my knowledge.

30.6.07

Dr. H. K. VERMA
Professor,
Department of Electrical Engineering,
Indian Institute of Technology Roorkee,
Uttaranchal - 247 667, INDIA.

DR. B. K. GANDHI
Professor,
Mechanical and Industrial Engg. Dept.
Indian Institute of Technology Roorkee
Uttaranchal - 247 667, INDIA.

ACKNOWLEDGEMENT

I am very indebted to my institution, **Indian Institute of Technology, Roorkee** for providing me opportunity to pursue my Masters. The lessons that this campus has taught are of immense value to me and I hope to cherish over the memories of this stay in the years to come.

Thanks to Head, Department of Electrical Engineering, Group leader and the team of **MEASUREMENT AND INSTRUMENTATION** for extending their co-operation in the academic proceedings.

Dr. H. K. VERMA, Professor, Department of Electrical Engineering, IIT Roorkee, my guide is the first person behind the success of this dissertation. "*Great men are as gentle as flowers and as strong as trees*", that is my guide. I frankly admit that this work evolved through substantial discussions with him. He was my motivation all through the work and had been a great encouragement at times when I stuck up. Man of his own kind, I salute to his perfection. For sure, learning under him is a unique experience.

I should be grateful to **Dr. B. K. GANDHI,** Professor, Dept. of Mechanical and Industrial Engg., IIT Roorkee, my co-guide, for his timely advices and support; he has given to me through out the work. I am very much an admirer of his enthusiasm and mingling nature. He has been a knowledge resource to me through out the work.

I thank **Sasank Patnayak, RESEARCH SCHOLAR, AHEC** for his valuable support and help he has given to me.

I am left indebted to all my friends, for letting their lives run beside mine for a while. They had always been a cheerful company to me. My gratitude to them cannot be expressed in words, i thank all my friends for rendering a ready help whenever I needed.

Dedicated

to

My Parents

ABSTRACT

Discharge measurement in a hydropower station is the most difficult and complex problem as it demands accuracy in measurement. For years the accuracy of flow measurement remained unsatisfying, until the high speed digital age took over the analog methods. An accurate measurement of water discharge rate using flow measurement devices can be ensured only by applying flow measurement devices correctly, which in turn requires the knowledge of the flow profile in the water channel. The velocity profiles developed in various geometries of trapezoidal open channel are found to be so complex, that the accurate measurement of these profiles is a tedious and challenging job. Though various flow measurement methods have been tried over the past 20 years, yet the accuracy demand has not been met so far.

In this dissertation work, a comparison of recently developed open channel flow measurement instrument Horizontal-Acoustic Doppler Current Profiler (H-ADCP) and traditional instrument Propeller Current Meter (PCM) have been done for three small hydro power stations in Punjab (India), the comparison reveals satisfactory performance of H-ADCP. Effort has been made to investigate the velocity profile for various trapezoidal geometries of open channels. Flow in nine geometrically different open channels has been simulated by using Computational Fluid Dynamic (CFD), and from simulated open channels data, average velocity has been computed and compared to evaluate the accuracy of discharge measurement. Efforts have also been made to investigate the effect of different values of power law exponent and cubic spline interpolation schemes on accuracy of discharge computation. Accuracy of average width discharge computational method has been compared for three simulated trapezoidal open channels. Prior to trapezoidal open channel simulation work, validation of CFD has been done by comparing the simulated results with field-measured data obtained with H-ADCP and PCM.

Two rectangular open channels have been simulated by CFD analysis and discussed effect of aspect ratio on velocity profile of rectangular open channel. Simulated velocity profile has been compared for logarithmic law, power law, and parabolic law.

CONTENTS

LIST OF FIGURES

LIST OF TABLES

CHAPTER 1
INTRODUCTION

1.1 Background

Measurement of the efficiency of a hydroelectric generating unit in a power station as per IEC-60041 requires an accurate measurement of discharge rate through the turbine. Since decades, traditional devices are used for flow measurement includes weirs, flumes, transit time acoustic meter and propeller current meters. Each of these devices has its own advantages and disadvantages. For example, weirs are easy to construct, but sediment build up below weir crest and submergence increase error in flow rate estimation. A multi path transit time acoustic meters may be accurate, but it is costly to install and maintain. Propeller current meters are well known for flow measurement in hydroelectric power station. IEC-60041 and ISO-748 standards recommend a matrix of propeller current meters for open channel flow measurement.

Now-a-days, horizontal-acoustic Doppler current profiler (H-ADCP) is becoming popular for open channel flow measurement. In fact, ISO-748 and IEC-60041 standards were accepted for flow measurement, the H-ADCP was not developed. Therefore, it is important to validate the H-ADCP measurements with propeller current meter measurements for the open channel flow. The flow profile in open channel changes according to the geometry. It is easy to handle rectangular open channels and therefore much of research work has been done with this type of channel geometry. However, flow measurement in trapezoidal open channel is not easy to handle and therefore, comparatively less work are observed in this area.

1.2 Introduction to CFD

Computational Fluid Dynamics (CFD) analysis could be used to model the channel and simulate the flow through it [1]. In Computational Fluid Dynamics (CFD), basic equations of fluid flow are used to model the physical world. In doing so, a number

of assumptions are made to simplify the problem. This allows a wide range of complex problems to be simulated using a computer. However, it is important to realize that CFD results are subjected to errors. In addition, there are situations in which the CFD analysis fails to produce results. With such cases, negative fluid densities may be encountered. So prior to CFD analysis validation of the software for typical problem is an inevitable part to confirm the reliability of the CFD analysis procedure.

The main feature of CFD is discretisation. This means that the volume to be analyzed is sub-divided into numerous smaller parts. These parts are known as *cells* and they joined to form a *mesh*. When CFD was first developed, these cells were usually had the shape of a rectangular block. However, modern CFD techniques allow cells of different shapes to be mixed and used. Even rhombic or tetrahedral shaped cells are possible.

Broadly, the strategy of CFD is to replace the continuous problem domain with a discrete domain using a grid. In the continuous domain, each flow variable is defined at every point in the domain. For instance, the pressure p in the continuous 1D domain shown in the Fig 1.1 below would be given as

$$p = p(x),\ 0 < x < 1$$

In the discrete domain, each flow variable is defined only at the grid points. Therefore, in the discrete domain shown below, the pressure would be defined only at the N grid points.

$$p_i = p(x_i),\ i = 1, 2, \ldots, N$$

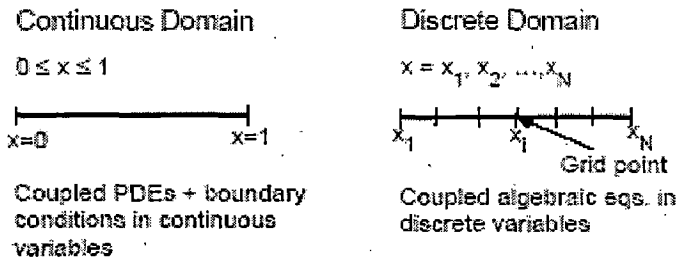

Fig 1.1 Continuous and discrete domain representation of pressure [1]

In a CFD solution, one would directly solve for the relevant flow variables at the grid points. The values at other locations are determined by interpolating the values at the grid points. The governing partial differential equations and boundary conditions are defined in terms of the continuous variables p, $\vec{V}$ etc. One can approximate these in the discrete domain in terms of the discrete variables p_i, $\overrightarrow{V_i}$ etc. The discrete system is a large set of coupled, algebraic equations in the discrete variables. Setting up the discrete system and solving it (which is a matrix inversion problem) involves a very large number of repetitive calculations and is done by the digital computer. This idea can be extended to any general problem domain.

1.3 Objectives of Dissertation

Briefly stated, following are the objectives of dissertation work:

- Comparison of H-ADCP and propeller current meters.
- Study the effect of aspect ratio on rectangular open channel flow profile and comparison of rectangular open channel flow profile and theoretical profile.
- Simulation of velocity profiles for various trapezoidal and semi-trapezoidal open channel geometries using CFD.
- Study the power law extrapolation and cubic spline interpolation techniques for discharge computation.
- Develop discharge computation method for trapezoidal channel.
- Identify the accurate methods for average velocity computation.

1.4 Organization of Dissertation Report

This dissertation report is organized as follows:

Chapters 1 and 2 introduce the dissertation work and open channel discharge measurement with H-ADCP and current meters.

Chapter 3 is devoted to comparison of H-ADCP and propeller current meters.

Chapter 4 introduces the basic steps involved in CFD analysis for open channel modeling and discusses validation procedure and the effect of aspect ratio on flow profile in rectangular open channel.

Chapter 5 presents the results of CFD simulations for various trapezoidal and semi trapezoidal open channel geometries and suggest the average velocity computation methods.

Finally, *chapter 6* concludes the report and puts forth the scope of further work that can be done as an extension of this dissertation work.

1.5 Literature Review

Doering and Hans (2001) have discussed the necessity of accurate flow measurement for developing the head-power-discharge relationship for low head hydroelectric power plant. They have used traditional current meters for collecting the array of velocity data and examined accuracy of velocity area method described by the German engineering standard.

Muste, et al. (2004) presented that moving vessel ADCP can successfully estimate river discharge and they reported that the small and large turbulence scales are smoothed out through a process similar to time averaging such that the output discharge equally samples the whole range of fluctuations; they also discussed assumptions and error sources involved in ADCP measurements using moving vessels

In an another work, Muste, et al. (2003) studied the external factor that might effect the accurate capturing of the mean and turbulence flow characteristics in rivers specially using fixed mounted ADCP measurements. They have discussed the relationship between the spatial and temporal characteristics of the instrument and the river turbulence scales at measurement site and effect of the length of sampling time adopted during measurement.

Juan, et al. (2000) observed that the accuracy of stream wise mean velocity measured by the fixed ADCP, affected by the temporal resolution of data. They have also discussed the averaging interval selection based on autocorrelation function (ACF).

Bland, et al. (2000) reported about accurate estimation of net residual discharge in tidally affected rivers or estuaries is possible by using ultrasonic instrument by calibrating the index velocity data measured by ultrasonic instrument, they discussed the uncertainty in flow measurement using vessel mounted ADCP.

Gonzalez, et al. (1996) carried out analysis of open channel flow using velocity data collected with an acoustic Doppler current profiler (ADCP). ADCP's have been utilized for field measurement and tested the reliability and accuracy of ADCP's by comparing the velocity profiles measured using ADCP with logarithmic and power law velocity distributions and from comparison, they have also estimated the shear velocity and roughness constant.

Sarma, et al. (2000) reported that the logarithmic law and parabolic law could be applied for mimic the velocity distribution in sub critical and supercritical flows in smooth and rough open channels. They have discussed that in some cases the vertical velocity profile at outer and inner zone can be modeled by logarithmic and parabolic law respectively.

Fenton, (2002) presented mathematical correlation for determining average velocity by two, three and four point velocity measurement at arbitrary depth in open channel cross-section and verified the result by comparing with traditional correlation.

CHAPTER 2

FLOW MEASUREMENT TECHNIQUES FOR OPEN CHANNELS

2.1 Basic Concept of Open Channel Flow

Flow can be classified into open channel flow and closed conduit flow. Open channel flow conditions occurs whenever the flowing stream has a free or an unconstrained surface that is open to the atmosphere. Flows in canals or in vented pipelines, which are not flowing full, are typical examples. The presence of the free water surface prevents transmission of pressure from one end of the conveyance channel to another as in fully flowing pipelines. Thus, in open channels, the only force that can cause flow is the force of gravity on the fluid. As a result, with steady uniform flow under free discharge conditions, a progressive fall or decrease in the water surface elevation always occurs as the flow moves downstream.

The actual distribution of flow velocity is generally quite complex. Open channel flow is often laminar or near laminar, with the different layers moving at different velocities. Flow velocity at the contact point with the channel boundary is low. Typically, the highest velocity flow is located in the center of the flow channel and slightly below the water surface. Fig 2.1 shows typical velocity profile or vertical velocity distribution under open channel flow conditions.

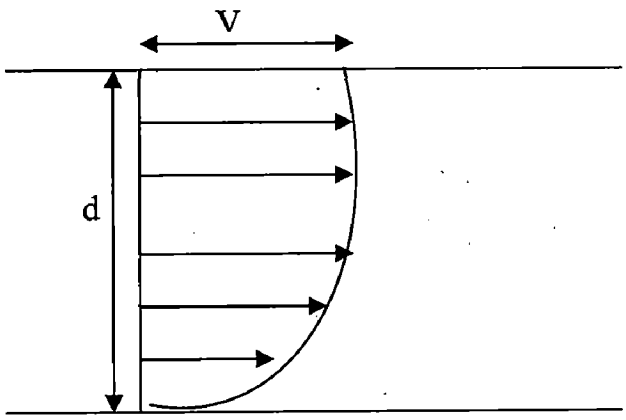

Fig 2.1 Typical velocity profile in open channel

A general knowledge of velocity distributions is extremely important in evaluating and selecting a method of flow measurement. Sites with irregular or complicated channel geometries, such as meanders or riffle areas, can cause a decrease in measurement accuracy when using methods that rely on velocity measurements to calculate discharge.

2.2 Velocity Measurement Devices

2.2.1 Principle of Propeller Current Meters

A current meter consists of a rotor or propeller mounted on a bearing and shaft. The fluid to be measured is passed through the housing, causing the propeller to spin with the rotational speed proportional to the velocity of the flowing fluid within the meter. A device to measure the speed of the rotor is employed to make the actual flow measurement. The sensor is generally an electronic type sensor that detects the passage of each rotor blade generating a pulse. The principle of the operation is based on the proportionality between the velocity of the water and the resulting angular velocity of the meter rotor.

By placing a current meter at a point in a stream and counting the number of revolutions of the rotor during the measured interval of time, the velocity of water at that point is determined. The number of revolutions of the rotor is obtained by an electrical circuit through the contact chamber. The current meter is put in the flow with the propeller axis parallel to the flow direction and the propeller peak against the flow. The rotational speed N, (Hz) of the propeller is a linear function of the flow velocity V, m/s in the measuring point [2, 3]:

$$V = (K) * N + B \tag{2.1}$$

where,

N= the number of pulses counted for a given preset time, Hz

K= Hydraulic Pitch of Propeller, m

B= Characteristics of Current Meter, m/s

The K and B are constants of the current meter and have to be determined by calibration.

2.2.2 Principle of H-ADCP

The H-ADCP uses sound to measure water velocity. The sound transmitted by the H-ADCP is in the ultrasonic range. The lowest frequency used by commercial H-ADCPs is around 30 kHz, and the common range used for the open channel measurements is between 300–3,000 kHz. The H-ADCP measures water velocity using a principle of physics discovered by Johann Doppler known as Doppler shift. Doppler's principle relates the change in frequency of a source to the relative velocities of the source and the observer [4]. Doppler shift can be defined as the apparent change in the frequency of a wave as sensed by an observer, due to the relative motion of the source and the observer. If the exact source frequency is known and the observed frequency can be calculated, equation 2.2 can be used to calculate Doppler shift due to the relative velocities of the source and observer.

$$F_D = F_s\left(\frac{V}{C}\right) \tag{2.2}$$

Where,

F_D= the Doppler shift frequency, in hertz.

C = the speed of sound, in m/s.

F_S = the transmitted frequency of the sound from a stationary source, in hertz.

V = relative velocity between the sound source and sound wave receiver, in m/s.

(I) Measuring Doppler Shifts From A Moving Platform

When the scatterers are moving away from the H-ADCP, the sound (if it could be perceived by the scatterers) shifts to a lower frequency. This shift is proportional to the relative velocity between the H-ADCP and the scatterers (Fig 2.2). Part of this Doppler-shifted sound is backscattered towards the H-ADCP, as if the scatterers were the sound source (Fig 2.2). The sound is shifted one time (as perceived by the backscatterer) and a second time (as perceived by the H-ADCP transducer) [4].

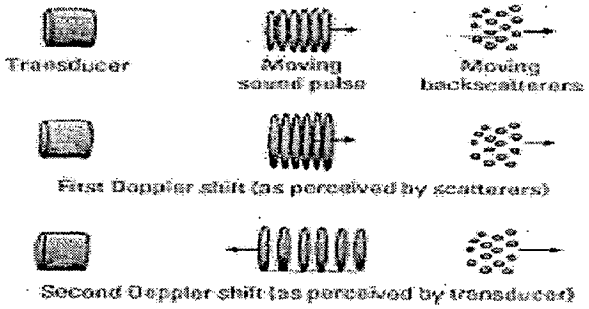

Fig 2.2 Reflected pulse showing two Doppler shifts [4].

Because there are two Doppler shifts, Equation 2.2 becomes:

$$F_D = 2 \cdot F_D\left(\frac{V}{C}\right) \tag{2.3}$$

Only radial motion, which is a change in distance between the source and receiver, will cause a Doppler shift. Mathematically, this means the Doppler shift results from the velocity component in the direction of the line between the source and receiver, as:

$$F_D = 2 \cdot F_s\left(\frac{V}{C}\right) \cdot \cos(\theta) \tag{2.4}$$

Where, θ is the angle between the relative-velocity vector and the line of the H-ADCP beam.

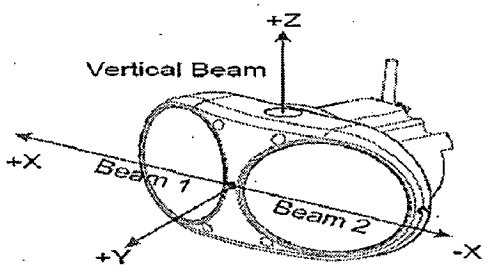

Fig 2.3 H-ADCP with beam orientations [5]

Normally the H-ADCP will be mounted in one sidewall of the channel normal to the flow. The H-ADCP will transmit two acoustic waves to the channel at angle of 10-15° at both sides of the normal (Fig 2.3). By comparing the reflected and the parent wave frequencies of the two acoustic beams, both the magnitude and the direction of flow can be estimated.

2.3 Methods of Determination of Channel Mean Velocity

The mean velocity of the flow in each vertical section can be determined by any of the following methods, depending on the time available and having regard to the width and depth of the water, to the bed conditions. The following methods are recommended by ISO-748 to determine mean velocities in a vertical section from the propeller current meters. In case of H-ADCP, same methods can be applied for determining the mean velocity in an open channel instead of in a vertical section of the channel. H-ADCP scans velocity at each predefined cells in a horizontal plane of measurement section. Average velocity, at different desired horizontal planes is determined by integration method or by simple averaging of measured data. For determining the average velocity in the channel, it is required to place propeller current meter at desired position at different vertical section, while H-ADCP scans the velocity at the number of vertical sections as number of cells defined for that transect. So that the time required for determining average velocity in an open channel will reduce.

2.3.1 Reduce Point Averaging Methods

Reduce point methods are as follow [6]:

(I) One-Point Method

Velocity observation shall be made on each vertical section by exposing the current meters at 0.6 of the depth below the surface. The value observed shall be taken as the mean velocity in the vertical. Alternatively, by exposing the H-ADCP at same position and it observes the average velocity, in a horizontal plane, which shall be taken as the mean velocity in the channel. Some authors have mentioned that 0.625 of the depth below the surface can give better accuracy as compared to 0.6 of the depth[7]. Accuracies of these two points are analyzed in next section of dissertation work.

(II) Two-Point Method

Velocity observations shall be made at each vertical or horizontal plane by exposing the current-meter or H-ADCP at 0.2 and 0.8 of the depth below the surface. The average of the two values shall be taken as the mean velocity in the vertical or an open channel.

(III) Three-Point, Five-Point And Six -Point Methods

In these methods, velocities are measured on each vertical or horizontal plane at various depth below the surface and as near as possible to the surface and the bottom. The mean velocity in a vertical or in an open channel may be determined from the following equations [6, 7]:

Three-point weighted method - $V_{(mean)} = 0.25 * (V_{0.2} + 2* V_{0.6} + V_{0.8})$

Three point method -$V_{(mean)} = 0.333 * (V_{0.2} + V_{0.6} + V_{0.8})$

Five-point method - $V_{(mean)} = 0.1* (V_{sur} + 3* V_{0.2} + 3* V_{0.6} + 2* V_{0.8} + V_{bed})$

Six Point method- $V_{(mean)} = 0.1* (V_{sur} + 2* V_{0.2} + 2*V_{0.4} + 2* V_{0.6} + 2* V_{0.8} + V_{bed})$

Four point method- $V_{(mean)} = 0.25* (V_{0.2} + V_{0.4} + V_{0.7} + V_{0.9})$

2.3.2 Vertical Velocity-Curve Method

The measurement of velocity by this method shall consist of velocity observations made at a number of points along the vertical between the surface and the bed of the channel. The spacing of the measuring points shall be so chosen that the difference of velocities between two adjacent points shall not be more than 20 percent w. r. t highest value of both. The mean velocity of that vertical and its position shall then be determined from the graph. The method is very accurate, depending upon the number of data points measured for profile, but is time consuming and costly. When the turbulent flow condition exists, the velocity curve can be extrapolated from the last measuring point to the bed or wall by calculating V_x from the equation: (m varies from 2 to 10)

$$v_x = v_a \left(\frac{x}{a}\right)^{\frac{1}{m}} \qquad (2.5)$$

where,

V_x = Point velocity in the extrapolated zone at a distance x from the bed or wall.

V_a = Velocity at the last measuring point at a distance a, from the bed or wall.

2.3.3 Integration Method

In this method, the current-meter is lowered and raised through the entire depth on each vertical at a uniform rate. The speed at which the meter is lowered or raised should not be more than 5 % of the mean water velocity and should not in any event exceed 0.04

m/s. Two complete cycles should be made on each vertical and if the results differ by more than 10 %, the operation (two complete cycles) should be repeated until results within this limit are obtained. This method is suitable for propeller-type current-meters and cup-type current meters and for electromagnetic current-meters, provided the vertical movement is less than 5 % of the mean velocity. The integration method gives good results if the time of measurement allowed is sufficiently long (60 s to 100 s) [8].

CHAPTER 3

COMPARISON OF H-ADCP AND PCM

The velocity distribution over a flow section is required to be measured for evaluating the flow through open channel. Horizontal Acoustic Doppler Current Profiler (H-ADCP) and Propeller Current Meters (PCM) are the instruments used in this work for acquiring the flow velocity at discrete position in the open channel measurement cross-section at three measurement sites. This chapter includes the comparison of H-ADCP and PCM, and validates the discharge measurement method of H-ADCP with respect to PCM, and developed methodology for estimating partial discharge in center of unmeasured zone.

A matrix of point velocity measurement is generally being carried out by fixing current meters at all the desired location or by using an array of current meters with the movement in horizontal or vertical direction. This is a laborious and time-consuming method. H-ADCP has been used in the present work for open channel flow measurement. It is very easy to install an H-ADCP in the open channel to scan the velocity distribution along width of channel with better spatial (cell size) and temporal (averaging interval) resolutions. A controlled movement of H-ADCP along the depth of the channel provides velocity matrix across the flow section. A comparison of flow rate measured by a horizontal array of propeller current meters and H-ADCP is carried out by using both instruments along the channel depth at three small hydropower stations in Punjab (India).

3.1 Requirements of Standards

Accuracy of discharge measurement in hydro power stations depends on selection of the measurement site and instruments. IEC-60041 and ISO-748 standards are recommended for improving accuracy of discharge measurement. IEC-60041 has mentioned basic requirements of propeller current meter and velocity measurement using propeller current meters. ISO-748 has mentioned basic requirements of measurement site selection.

3.1.1 Requirements of IEC 60041

The basic requirements of an open channel flow measurement by Propeller Current Meters (PCM) are presented below [8].

(I) Duration of Measurement

Measurements for each current meter position shall last at least 2 min. If variation in the water velocity is present, the measurement over cross-section shall include at least four cycles of these variations. This may produce influence on the entire test measurement.

(II) Number of Measuring Points

The number of current meters shall be sufficient to ensure a satisfactory determination of the velocity profile over the whole measuring section. A single point measurement is not permitted under this standard. At least 25 measuring points shall be used in a rectangular or trapezoidal section. If the velocity distribution is likely to be non-uniform, the number of measuring points, Z, shall be determined from equation (3.1).

$$24\sqrt[3]{A} < Z < 36\sqrt[3]{A} \tag{3.1}$$

where,

A is the area of measuring section, in square meter.

If the conduit or channel is divided into several sections, measurement shall be made simultaneously in all sections.

(III) General Requirement of Current Meters

The current-meter propeller shall not be less than 100mm diameter except for measurements in the peripheral zone where propellers, as small as 50mm, may be used. The distance from trailing edge of the propeller to the leading edge of the mounting rod shall be at least 150mm.The angle between the local velocity vector and the axis of the current meter should not exceed 5 degrees. When larger angles are unavoidable, self-compensating propellers, which measure directly the axial component of the velocity shall be used, but only at angles, for which they have been designed and calibrated.

(IV) Distribution of Measuring Points

Measuring points shall be closer to one another in the zones of steeper velocity gradient. Points shall be normally spaced so that the difference in velocity between two adjacent points does not exceed 20% of the greater of two velocities.

3.1.2 Requirements of ISO-748

As recommended by ISO-748, the accuracy of discharge measurement is increased if the measurement site satisfies the following conditions [6]:

i. The channel at the measuring site should be straight and of uniform cross section and slope in order to minimize abnormal velocity distribution.

ii. The bed and margins of the channel should be stable and well defined at all stages of flow in order to facilitate accurate measurement of the cross-section and ensure uniformity of the conditions during and between discharge measurements.

iii. Flow directions at all points on any vertical across the width should be parallel to one another and at right angles to the measurement section.

iv. Conditions at the section and in its vicinity should also be such as to preclude changes, taking place in the velocity distribution during the period of measurement.

v. The depth of water at the section should be sufficient for all stages to provide the effective immersion of the current-meter (ideally, depth should be greater than eight times the diameter of the propeller).

vi. Sites displaying vortices, reverse flow or dead water should be avoided.

vii. Sites where there is converging or diverging flow should be avoided.

If the measurement site satisfies above requirement then it may be possible to reduce the number of verticals and to allocate equal distance spacing between the verticals. The verticals should be chosen so that the discharge in each segment is less than 5% of the total in so far as possible, and such that in no case should it exceed 10 %.

3.2 Measurement Procedure

For the comparison of intrusive and non-intrusive instruments PCM and H-ADCP respectively, the matrix of velocity data in cross-section of low headrace channel was collected at three small hydro power stations 1 x 1000 KW, 2x1000KW and 2x1000KW at Punjab in India. The velocity data were collected by placing H-ADCP in downstream around 5 meters away from the position where PCM structure was mounted. The

measurement were not carried out simultaneously but tried to maintain same water head in both cases. According to ISO-748 an array of propeller current meters was attached to a movable frame, designed to move up and down for velocity measurement at desired depth of 0.4m, 0.8 m, 1.2 m, and 1.6 m from the water surface, and according to IEC-60041 arrays of PCM were placed at different vertical and horizontal position that is mentioned above in standard requirements. Each point's velocity was measured at 120-second average intervals and such four sets of data was averaged for getting accurate velocity at each point in the cross-section of three hydropower stations.

3.2.1 Data Acquisition with the H-ADCP

For data acquisition, the communication between H-ADCP and PC has to be established through RS-232 serial port as shown in Fig 3.1. This is done with the help of BBTalk (provided by H-ADCP manufacturers). After communication is established successfully, proper mounting of the H-ADCP is done and real time data is monitored and acquired using WinH-ADCP [5].

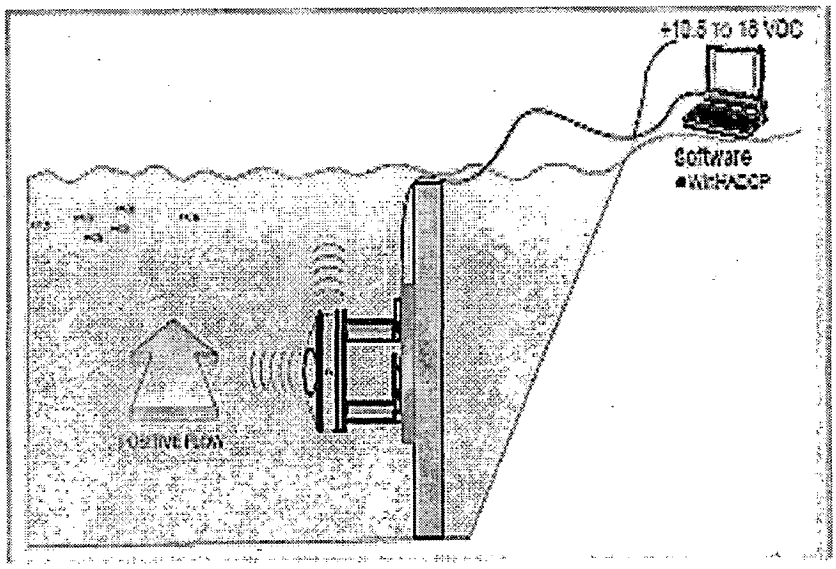

Fig 3.1 H-ADCP mounting layout in open channel [5]

(I) Communication Parameters

Before establishing communications with the H-ADCP, *BBTalk* must be configured [5].

i. At the Connect to screen, select the H-ADCP type (WorkHorse, Broadband, Narrowband, Channel Master, or NEMO) from the list.

ii. Select the COM Port, the H-ADCP is connected to Click Next (Shown in Fig 3.2).

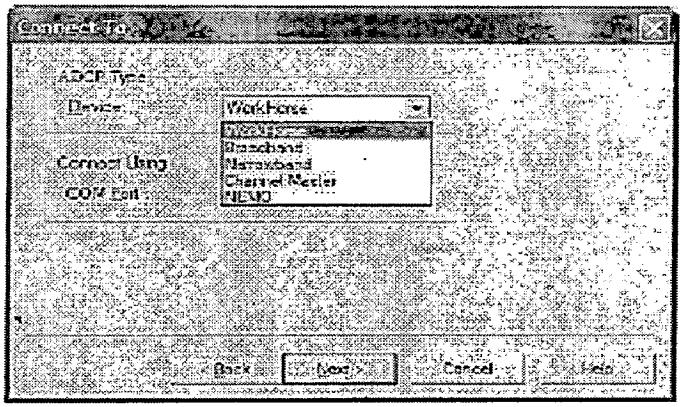

Fig 3.2 BBTalk- connect to screen

iii. On the Port Settings screen, select the baud rate, parity, stop bits and flow control. Click Next shown in Fig 3.3.

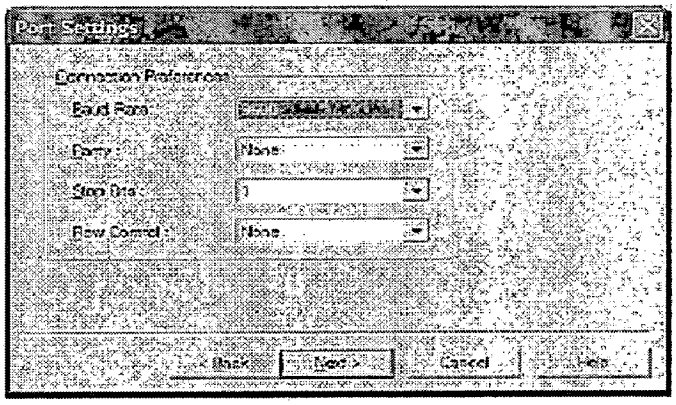

Fig 3.3 BBTalk-port settings screen

iv. On the Options screen, select the desired settings. As Shown in Fig 3.4.

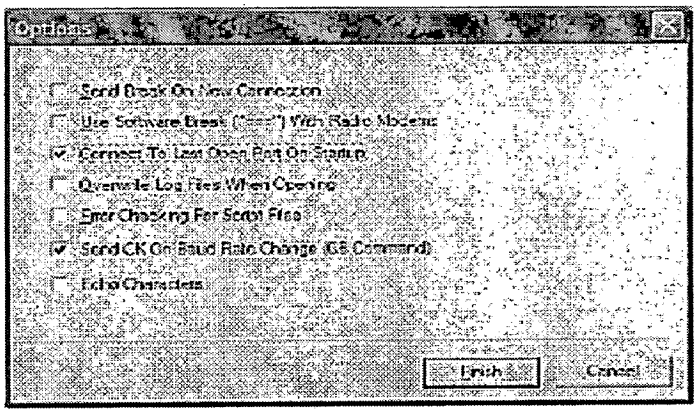

Fig3.4. BBTalk-options screen

v. Click Finish.

vi. On the File menu, click Break. The following wakeup message appears on the log file window. Shown in Fig 3.5

xxxxxx H-ADCP

RD INSTRUMENTS (c) 1997-2002

ALL RIGHTS RESERVED

Firmware Version xx.xx >

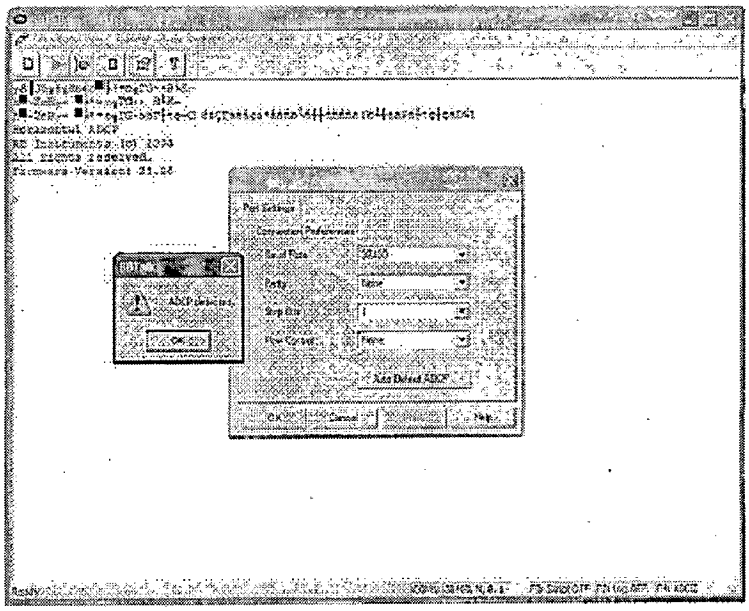

Fig 3.5 BBTalk-auto detect

vii. Click OK when the H-ADCP is detected. Try to wakeup the WorkHorse again.

(II) H-ADCP Mounting

H-ADCP was also attached to movable frame and placed at same different horizontal position at where PCM was placed. H-ADCP is accurately mounted at normal to direction of flow with the help of WinH-ADCP, while PCM is direction insensitive. Therefore according to IEC-60041 standard, if the angle between rotational axis of PCM and flow direction is greater than 5° than it gives erroneous result. Basic process of H-ADCP mounting with the help of software is given below.

WinH-ADCP can help with the physical mounting of an H-ADCP by causing it to ping and displaying real time orientation, depth, and temperature data in a large font.

i. Start *WinH-ADCP*.

ii. On the Start Screen, click Mount H-ADCP.

iii. On the Communications Settings screen (see Fig 3.6), enter the communications settings for the H-ADCP. If you are unsure of the setting, use the Auto Detect button.

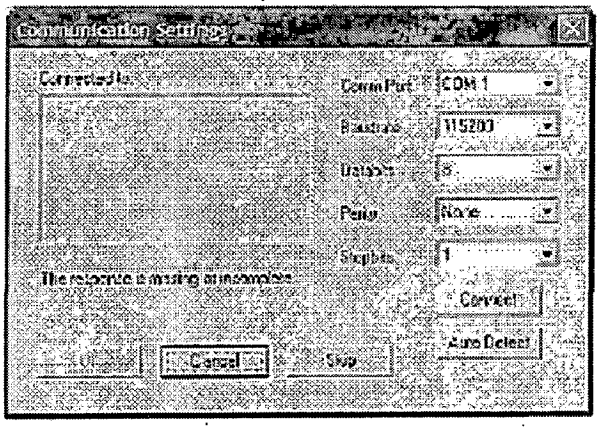

Fig 3.6 Communications setting screen

iv. The Sensors screen of the *WinH-ADCP* software indicates the pitch and roll angles of the H-ADCP as shown in Fig 3.7. Adjust the mount until the roll is zero. The H-ADCP rolls about the Y-axis. The roll must be zero. Adjust the mount until the pitch is zero. The H-ADCP pitches about the X-axis.

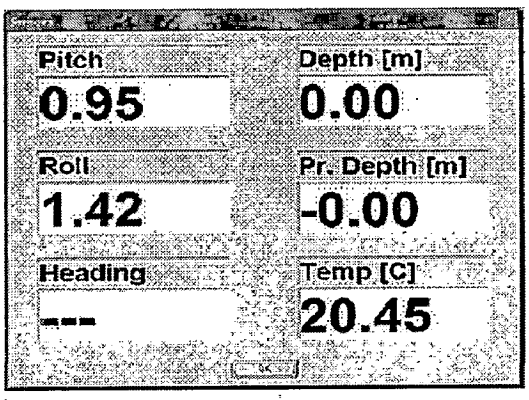

Fig 3.7 Sensors screen

(III) Real Time Data Acquisition

Accuracy of acquired velocity data depends on operating setting of the H-ADCP. Before start H-ADCP software in data acquisition mode, operating setting of the H-ADCP should be defined according to open channel dimension and flow characteristics. At three SHP station, the matrix of velocity data was collected at sampling frequency of

0.1 Hz. Sampling interval and average interval was selected according turbulence in flow [9]. The water flow at three SHP was uniform. Therefore, averaging interval was taken 360 seconds. The H-ADCP does not measure velocity at single point; it measures the velocities throughout the horizontal plane of the measurement section and divides the horizontal plane into uniform segment (cells or bins). Therefore, it is important to define the number of cells according to width of the channel and size of cell. At three SHP station, operating setting of 600 kHz H-ADCP was defined as given below in Table 3.1[10, 11, 12, 13]

Table 3.1 Operating setting of 600 kHz H-ADCP

Spatial resolution(Cell size):	**0.5 meter**
Number of cells:	50
Unmeasured zone :	2 meter (blank distance + half of bin)
Averaging interval:	360 seconds
Sampling interval :	10 seconds

Once operating condition is defined, *WinH-ADCP* was started in the Data Acquisition mode, before it communicates with the H-ADCP, must be set up as given below [5].

i. Connect and power up the H-ADCP using 12V DC.
ii. Start *WinH-ADCP*. If *WinH-ADCP* is already running, on the Configure menu, click Setup Wizard. On the Start dialog, click Real-Time Data Acquisition.
iii. On the Communications Settings dialog box, select the COM Port, Baud rate, Data bits, and Stop bits. If you are unsure of the setting, use Auto Detect. Once setup has been completed, *WinH-ADCP* will remember these setting and automatically connect the H-ADCP the next time the program is started. To skip connecting to the H-ADCP, click the Skip button.
iv. *WinH-ADCP* will connect to the H-ADCP and confirm the communication setting. When connected to box, the H-ADCP wakeup message is seen.
v. Click OK to continue to the Real-Time Data Acquisition screen

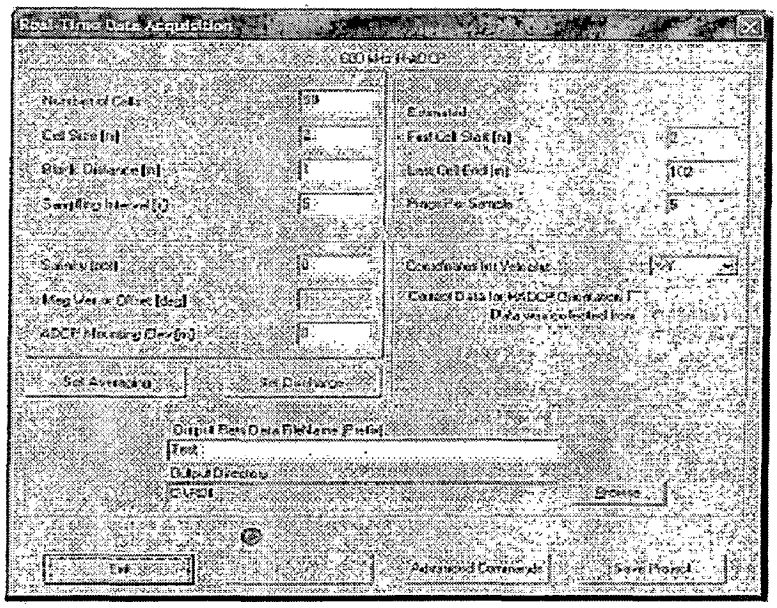

Fig 3.8 Real-time data acquisition screen

vi. Once the Real-Time Data Acquisition screen is setup, click the Save Workspace button to save the discharge and averaging settings. As Shown in Fig 3.8

vii. Click Acquire to begin data collection.

H-ADCP scans longitudinal and lateral directional velocity component while PCM measures only longitudinal direction velocity. The reliability of measured velocity data by H-ADCP can be tested by continuously monitoring the echo intensity of transmitted beams in H-ADCP virtual window. If intensity of beams are constant than measured data are accurate otherwise it may not be accurate due to external interference. Velocity data were collected from H-ADCP by play backing the H-ADCP software.

3.3 Discharge Computation Method

The various open channels discharge computation methods are given in Fig 3.9 as per ISO-748 standard.

The velocity depth integration graphical method for the open-channel discharge computation using the propeller-current meters is given below, as recommended by ISO-748. It is used in later part of the chapter for discharge computation.

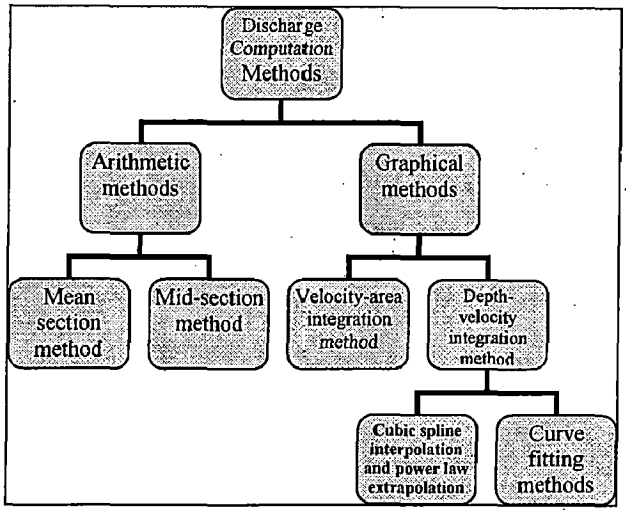

Fig 3.9 Discharge computation methods

3.3.1 Depth-Velocity Integration Method

Velocity observations are made at a number of points along the vertical between the surface and the bed of the channel. The spacing of the measuring points shall be so chosen that the difference of velocities between two adjacent points shall not be more than 20 percent of the higher value of the two. The velocity at each vertical section should be plotted against depth as shown in Fig 3.10 by using curve-fitting methodology or by using some interpolation scheme [6, 14].

(I) Cubic Spline Interpolating Scheme

In this approach, a set of cubic spline functions is used for velocity distribution approximation. Spline functions are partial polynomial functions that are connected in measuring points and have the same first and second derivative in this point. The algorithm using a set of cubic spline functions is very stable for unlimited number of measuring points and for any distance distribution of measuring points throughout the cross-section. The cubic spline provides an exact fit to the data as compare to other methods and overcome the problem like as over fitting data with higher polynomials [15, 16]. The data is interpolated in the interpolating range and extrapolation can be done to find the surface velocity of the channel. This method of cubic spline interpolation is most

commonly considered which is used for finding the velocity distribution in the vertical transect and horizontal velocity profile along the width of the channel [6].

(II) Power Law Extrapolation Scheme

There are two methods used for extrapolation of the velocity data into unmeasured zone. In the First method if unmeasured zone is less than 1 or 1.5 meter, the velocity distribution in unmeasured zone is assumed to follow the power law extrapolation. When the turbulent flow condition exists, according to the first method the velocity curve can be extrapolated from the last measuring point to the bed or wall (unmeasured zone) by calculating v_x from the equation 2.5 [6].

Second method if unmeasured zone is larger than 1 or 1.5 meter then power law extrapolation gives erroneous result. Therefore, mean velocity in middle of unmeasured zone is estimated from measured mean velocity in the channel as given in equation 3.2 and from this mean velocity at middle of unmeasured zone is extrapolated from this point to wall or bed of channel in same way as specified in first method . For both the case the selection of exponent constant m is important parameter.

$$\bar{V}_x = \frac{m}{m+1}\left\{\frac{d}{a}\right\}^{\frac{1}{m}} V_a \qquad (3.2)$$

where,

m is an exponent.

d is the total depth of flow, in meter.

Generally m lies between 2 and 7 but it may vary over a wider range depending on the hydraulic resistance. The value m=2 applies to coarse beds or walls while m=10 is characteristic of smooth beds or walls.

The unit-width discharges ($\bar{V} \cdot d$) of each vertical are interpolated and extrapolated nearer to sides walls. The total discharge through the channel is determined by integrating unit-width discharge with respect to width of the channel, as given in equation 3.3.

Total discharge is:

$$Q = \int q_i db \quad \text{Or} \quad Q = \sum \bar{V}_i d_i \Delta B \qquad (3.3)$$

where,

Q is the total discharge in an open-channel, m^3/s

$\bar{V}_i$ is the average velocity of the i^{th} vertical, m/s.

d_i is the depth of the i^{th} vertical, m.

ΔB is the incremental width along the channel, m

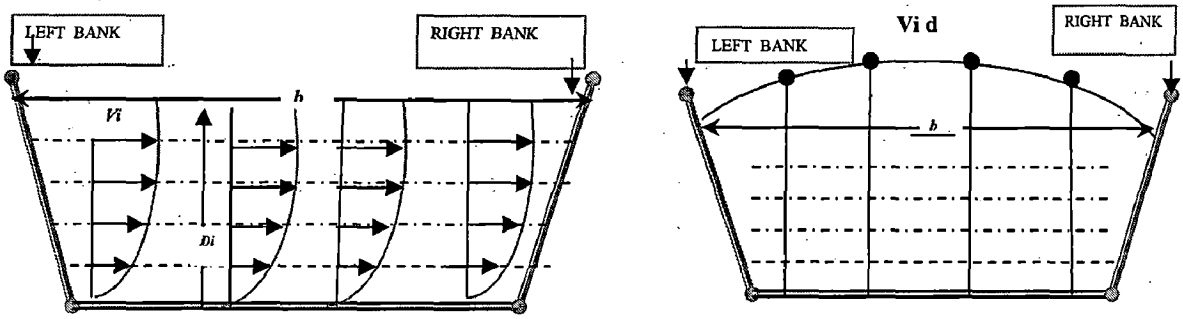

Fig.3.10 (a) Velocity vs. depth (b) Partial discharge vs. width profile

Horizontal Acoustic Doppler Current profiler (H-ADCP) has not been standardized for open channel flow measurement, But H-ADCP is becoming popular for open channel flow measurement. H-ADCP scans the flow rate at each predefined cell in horizontal plane of the channel cross-section. H-ADCP samples the velocity data at each cell and stores the ensemble velocity reading at center of the cell. The matrix of velocity data is read from H-ADCP by play backing data file, from that velocity data, discharge can be computed same way as methodology recommended for PCM by ISO-748. Comparison of the H-ADCP and PCM is carried out by determining the velocity at same locations in the cross-section of channel.

3.4 Results and Discussion

At 1x1000kw SHP station, the headrace channel cross-section 2.3 m deep and 19.44m wide, and matrix of 4x12 and 4x33 point's velocity was measured by PCM and H-ADCP respectively. Velocity data measured at number of vertical sections of the measurement cross-section by PCM is given Table 3.2. Velocity data was acquired at four depths through out cross-section. Detail of measurement procedure has been discussed in section 3.2. At 2x1000kw SHP station, the headrace channel cross-section

2.12 m deep and 19.37m wide, and matrix of 4x11 and 4x32 point's velocity was measured by PCM and H-ADCP respectively. At 2x1000kw SHP station the headrace channel cross-section 2.007 m deep and 10.8m wide, and matrix of 4x6 and 4x15 point's velocity was measured by PCM and H-ADCP respectively.

Table 3.2 Velocity data measured by PCM at 1x1000kw SHP

depth/ width	2.01	3.42	4.805	6.18	7.59	10.42	11.80	13.19	14.58	15.97	17.39
0.4	1.189	1.174	1.166	1.218	1.28	1.269	1.262	1.283	1.25	1.14	1.126
0.8	1.21	1.156	1.161	1.179	1.293	1.256	1.248	1.285	1.268	1.214	1.149
1.2	1.194	1.147	1.163	1.18	1.272	1.232	1.228	1.27	1.264	1.246	1.193
1.6	1.13	1.143	1.214	1.22	1.258	1.214	1.204	1.247	1.258	1.257	1.16

Vertical profile of average velocity and horizontal profile of partial discharge are created from measured velocity data. That is given in Fig 3.11, Fig 3.12 and Fig 3.13. It is created by above discussed velocity-depth integration discharge computation methodology that is implemented in MATLAB. As shown in Fig 3.11, Fig 3.12 and Fig 3.13 the interpolation of horizontal profile is smoothly carried out for H-ADCP data as compared to PCM data. However, accuracy of discharge measurement is affected by area of unmeasured zone, if the unmeasured zone is more than 1.5 or 2m, the power low extrapolation may fail to predict the velocity in unmeasured zone. For reducing the effect of unmeasured zone, the mean velocity $\overline{V}_x$ in middle of unmeasured zone has been estimated from mean of measured velocity data in the channel as given in equation 3.2, as recommended by ISO-748[3]. The accuracy of estimated average velocity depends on the selection of power law exponent m. An H-ADCP can accurately measure the velocity data nearer the opposite side wall of the H-ADCP mounted side. Therefore, the average velocity of last measured vertical by H-ADCP is compared with estimated average velocity V_x from computed average velocity V_a of measured data by using PCM or H-ADCP. From that comparison value of power law exponent can be determined for that channel. Generally m lies between 2 and 7 but it may vary over a wider range depending on the hydraulic resistance. The value m=2 applies to coarse beds or walls while m=10 is characteristic of smooth beds or walls. From equation (3.2), power law exponent m =4 has been determined for opposite side wall of H-ADCP mounted side. At three SHP

station, the side walls and bottom were concrete structured, so that power law exponent m = 4 has been used for power law extrapolation at solid boundaries. And the estimated mean velocity at middle of unmeasured zone is extrapolated to wall or bed of the channel by power low extrapolation as mention in section 3.3.1.

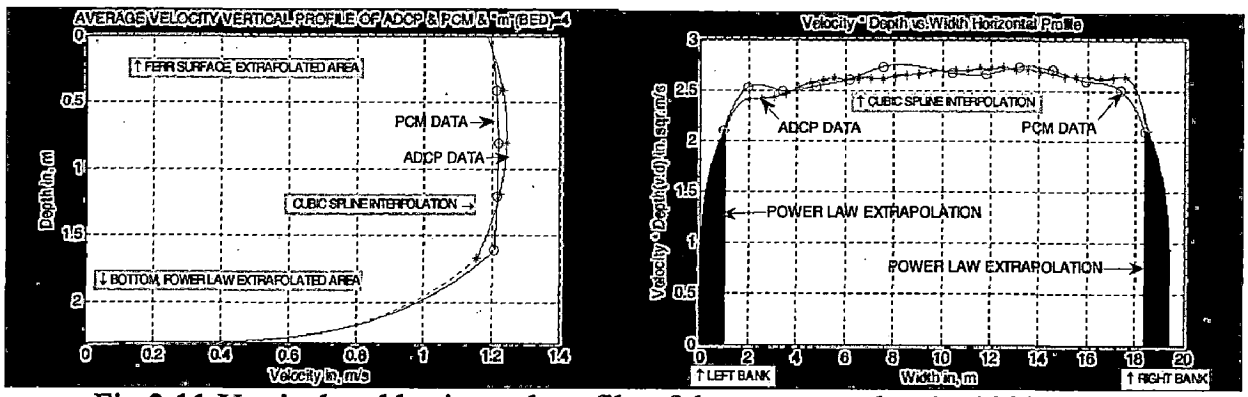

Fig 3.11 Vertical and horizontal profile of data measured at 1x 1000kw SHP

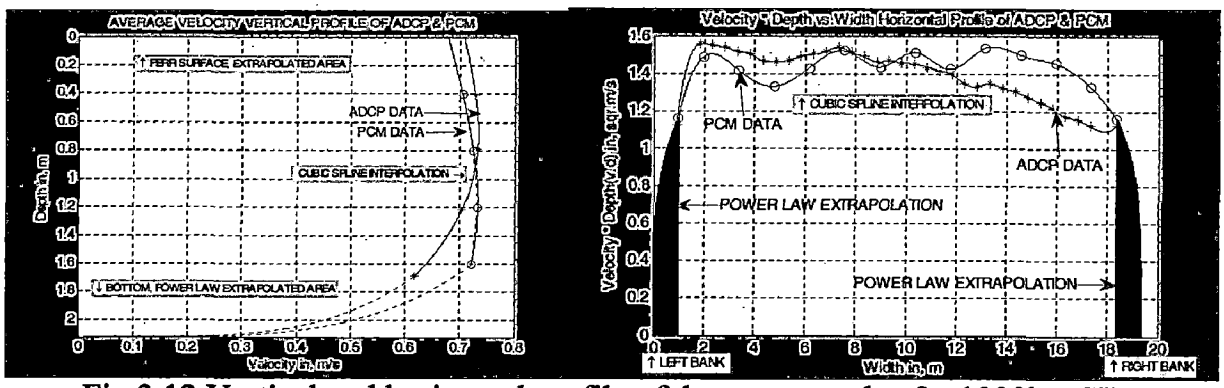

Fig 3.12 Vertical and horizontal profile of data measured at 2x 1000kw SHP

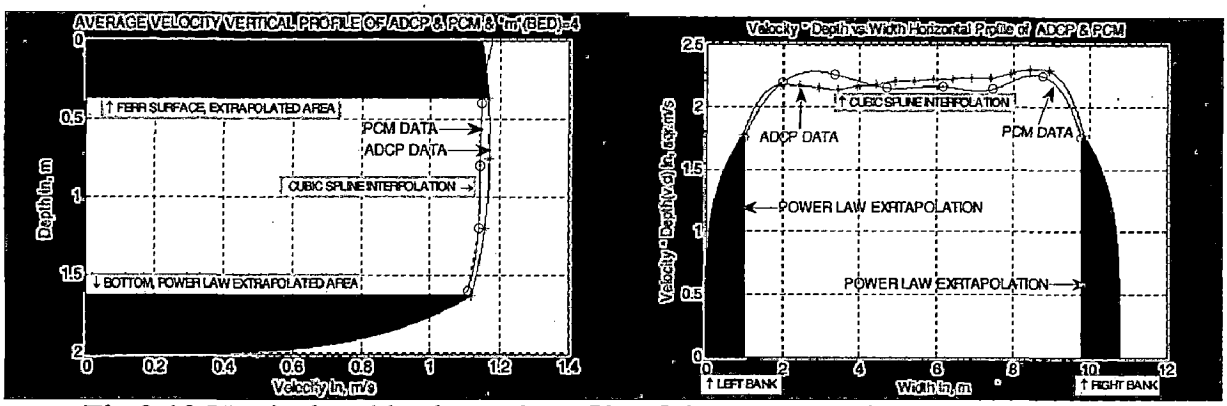

Fig 3.13 Vertical and horizontal profile of data measured at 2x 1000kw SHP

From the vertical and horizontal profiles, the variation in velocity data measured by PCM is more as compared to H-ADCP data, because of

i. The measurement was carried out by using different propeller current meters.

ii. Deviation in calibration from one PCM to another PCM model

iii. Due to the intrusiveness of PCM.

iv. Directional error in PCM.

Theoretically, the velocity measured by each PCM is analogous to the velocities measured at the center of H-ADCP bins. However, the analogy between a series of PCMs and an H-ADCP profile is not perfect. The PCM measure water velocity at individuals points in the vertical profile, whereas H-ADCP measures velocity at each cells, are really the center weighted mean of velocities that are measured throughout sample window. Therefore, H-ADCP gives velocity information in whole cross-section except unmeasured zone that is due to the blanking distance plus area of the transducer face into the water and on opposite side due to side lobe interference [3].

(I) Deviation Calculation

From above theoretically analysis, the H-ADCP is more accurate as compared to PCM. Therefore, deviation in discharge is determined with reference to H-ADCP. As given in Table 3.3, it is observed percentage deviation around ± 2.5%. The percentage deviation was calculated as:

$$\%\text{deviation} = \frac{(Q_{pcm} - Q_{adcp})}{Q_{adcp}} \times 100 \qquad (3.4)$$

Table 3.3 Percentage deviation in discharge computed from measured data

SHP	DEVICE	TOTAL DISCHARGE, m^3/s	AVERAGE VELOCITY, m/s	% DEVIATION
1X1000KW	H-ADCP	52.758108	1.183607	--
	PCM	53.281083	1.195339	0.996240
2X1000KW	H-ADCP	26.003604	0.633239	--
	PCM	26.449378	0.648965	2.483401
2X1000KW	H-ADCP	22.107239	1.021095	--
	PCM	21.844918	1.007811	-1.300952

Velocity data of 1x1000kw small hydropower station are further used for validating flow simulation procedure in CFD.

CHAPTER 4

OPEN CHANNEL FLOW SIMULATION BY CFD AND VALIDATION

The velocity profile developed in various open channel field conditions is found to be different from each other depending on the size and shape of the cross-section of the channel. Accurate measurement of discharge in these conditions is a challenging and tedious job. Accuracy of measurement is very much affected by the number of horizontal section or by the number of point's velocity in a vertical in the channel to obtain these profiles. Therefore, for minimizing the measurement errors and uncertainty in discharge measurement, placement of the flow meters across the cross-section of the channel should be precise. Experiments only permit data to be extracted at a limited number of locations in the open channel cross-section. In such a situation, the flow meters can be efficiently placed by the knowledge of expected velocity profile. Therefore, a general awareness about the expected profiles in various channel geometries is desirable for reducing the uncertainty in measurement. CFD allows the analyst to examine a large number of locations in the region of interest, and yields a comprehensive set of flow parameters for analysis.

By placing the flow meter (ADCP) at the prescribed number of level of the channel, it should be possible to trace out the variation in velocity profiles. The number of horizontal section for scanning the velocity will vary as the cross-section of the channel changes. IEC-41 provides the guidelines for placing PCM; same standard can be applied for placing the ADCP at different elevation.

Error in open channel flow discharge measurement is mainly due to extrapolation in unmeasured zone nearer to solid boundaries and free surface with lack of knowledge regarding the basic shape of velocity profile. Therefore, it is important to analyze the velocity profile nearer to solid boundaries and free surface. Maximum velocity point in the channel is changed according to aspect ratio (width/depth) of the channel. In later section of the chapter, flow simulation of simple narrow and wide rectangle open channel is done, which is compared with theoretical

data and coefficient of well-defined mathematical model is determined for simulated rectangular channels.

4.1 Computational Methodology

4.1.1 Governing Equations

Computational Fluid Dynamics (CFD) is the science of predicting fluid flow, heat transfer, mass transfer, chemical reactions, and related phenomena by solving mathematical equations that represent physical laws, using a numerical process.

Applying the fundamental laws of mechanics to a fluid gives the governing equations for a fluid. The conservation of mass equation is given in equation 4.1.

$$\frac{\partial \rho}{\partial t} + \nabla.(\rho \vec{V}) = 0 \tag{4.1}$$

In addition, the conservation of momentum equation is:

$$\rho \frac{\partial \vec{V}}{\partial t} + \rho\left(\vec{V}.\nabla\right)\vec{V} = -\nabla P + \rho \vec{g} + \nabla.\tau_{ij} \tag{4.2}$$

These equations along with the conservation of energy equation form a set of coupled, nonlinear partial differential equations. It is not possible to solve these equations analytically for most engineering problems. However, it is possible to obtain approximate computer-based solutions to the governing equations for a variety of engineering problems. This is the subject matter of Computational Fluid Dynamics (CFD). Fluent is a Finite Volume based code for fluid flow simulations [17].

4.1.2 Stages of CFD Analysis

Stage 1 Modeling Geometry: As shown in Fig 4.1, the first step in performing a CFD analysis is to create the shape of the fluid that needs to be analyzed. This can be done usually with the help of a standard CAD program or GAMBIT etc. It is easily possible to import data generated by such programs into a CFD package.

Stage 2 Meshing: In the second stage, the fluid is then sub-divided into numerous cells. This can be thought of as being similar to the way in which a Rubics Cube is divided into smaller bits. In many CFD packages, meshing can be done while the

shape is being defined. For such cases, it is common to have the first two stages performed simultaneously.

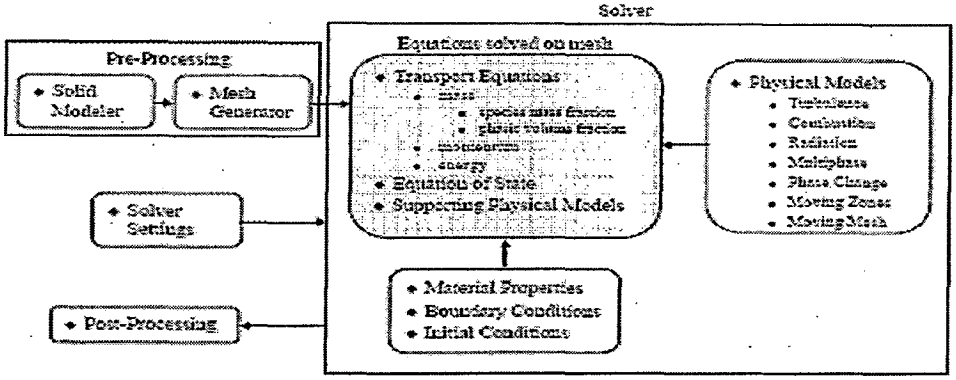

Fig. 4.1 Overview of CFD modeling

Stage 3 Preprocessing: Once meshing has been completed, boundary conditions are then applied to the fluid. This generally means specifying known velocities or pressures at specific points of the fluid. These initial conditions are what the computer uses to calculate the velocities and pressures in other parts of the fluid volume.

Stage 4 CFD Analysis: This step involves using a computer to solve mathematical equations of fluid motion. It is very intensive and usually requires the computer to solve many thousands of equations. In each case, the equations are integrated and boundary conditions are applied to it. This is known as equation discretisation and is applied to each individual cell of the mesh. The process is repeated in an iterative fashion until a required accuracy is achieved.

Stage 5 Post Processing: Post processing is done to make sense of the data generated by the CFD analysis. In solving the equations, a computer would have generated a fair amount of data for each cell. Since there are typically several thousand cells in a mesh, the total amount of data we are looking at here is enormous - definitely, an engineer would not like to browse through! Using the post processor, the results are easily sorted by a computer. It may then be displayed to the engineer as a graph. This usually has little arrows and contours that are much easier to understand. In such graphs, colors are used to differentiate between the different sizes of the values.

CFD package used in this work is FLUENT and the geometry creation is done using GAMBIT

4.2 Boundary Conditions and Solution Procedure

Simulation of open channel flow is carried out in two steps, (1) Modeling the measurement site and discretise it. That can be done in GAMBIT or CAD. (2) Solving the numerical equation at each node with initialization of boundary condition. That can be done in FLUENT and iterate it in fluent with predefined convergence criteria.

4.2.1 Geometry Modeling in Gambit

Steps involved in GAMBIT as following:

(I) Creating The Geometry

When click the **Geometry** command button on the **Operation** tool pad, GAMBIT opens the **Geometry** sub pad. The **Geometry** sub pad contains command buttons that allow creating, moving, copying, modifying, summarizing, and deleting vertices, edges, faces, and volumes. The **Geometry** sub pad also contains a command button that allows performing operations involving groups of topological entities.

(II) Meshing The Model

The **Mesh Volumes** command allows you to create a mesh for one or more volumes in the model. When you mesh a volume, GAMBIT creates mesh nodes throughout the volume according to the currently specified meshing parameters. To mesh a volume, you must specify the following parameters:

i. Volume(s) to be meshed
ii. Meshing scheme
iii. Mesh node spacing
iv. Meshing options

The meshing scheme used for this study is hexahedral for simple rectangle channels and tetrahedral for curved and trapezoidal channels.

(III) Specifying Zone Types

Zone-type specifications define the physical and operational characteristics of the model at its boundaries and within specific regions of its domain. There are two classes of zone-type specifications: 1. Boundary types 2. Continuum types

Boundary-type specifications, such as WALL or VENT, define the characteristics of the model at its external or internal boundaries. Continuum-type specifications, such as FLUID or SOLID, define the characteristics of the model within specified regions of its domain.

4.2.2 Simulation Procedure in Fluent

(I) Setting The Parameters

FLUENT can model the effects of open channel flow (e.g., rivers, dams, and surface-piercing structures in unbounded stream) using the VOF formulation and the open channel boundary condition. These flows involve the existence of a free surface between the flowing fluid and fluid above it (generally the atmosphere).

In such cases, the wave propagation and free surface behavior becomes important. Flow is generally governed by the forces of gravity and inertia. This feature is mostly applicable to marine applications and the analysis of flows through drainage systems. Using the VOF formulation, open channel flows can be modeled in **FLUENT**. To start using the open channel flow boundary condition, perform the following [1, 17]:

i. Turn on gravity.
   (a) Open the **Operating Conditions** panel.
   Define → Operating Conditions...
   (b) Turn on **Gravity** and set the gravitational acceleration fields.
ii. Enable the volume of fluid model.
   (a) Open the **Multiphase Model** panel.
   Define → Models → Multiphase...
   (b) Under **Model**, turn on **Volume of Fluid**.
   (c) Under **VOF Scheme**, select Implicit, **Explicit**, or **Geo-Reconstruct**.
iii. Under **VOF Parameters**, select **Open Channel Flow**.

Table 4.1 Open channel boundary parameters for the VOF model.

Boundary Type	**Parameter**
Velocity inlet	Flow Specification Method; Velocity Magnitude: Flow Direction
Outlet vent	Outlet Group ID: Pressure Specification Method; Free Surface Level; Bottom Level
mass flow inlet	Inlet Group ID; Secondary Phase for Inlet; Free Surface Level; Bottom Level

(II) Defining The Boundary Conditions

In order to set specific parameters for a particular boundary for open channel flows, the **Open Channel Flow** option should be turn on in the corresponding boundary condition panel. Table 4.1 summarizes the types of boundaries available to the open channel flow boundary condition, and the additional parameters needed to model open channel flow.

Defining Inlet Groups: Open channel systems involve the flowing fluid (the secondary phase) and the fluid above it (the primary phase).

If both phases enter through the separate inlets (e.g., inlet-phase2 and inlet-phase1), these two inlets form an inlet group. This inlet group is recognized by the parameter **Inlet Group ID**, which will be same for both the inlets that make up the inlet group. On the other hand, if both the phases enter through the same inlet (e.g., inlet-combined), then the inlet itself represents the inlet group.

Defining Outlet Groups: Outlet-groups can be defined in the same manner as the inlet groups.

Setting the Inlet Group: For pressure inlets and mass flow inlets, the **Inlet Group ID** is used to identify the different inlets that are part of the same inlet group. For instance, when both phase enter through the same inlet (single face zone), then those phases are part of one inlet group and the **Inlet Group ID** would set to 1 for that inlet (or inlet group).

In the case where the same inlet group has separate inlets (different face zones) for each phase, then the **Inlet Group ID** will be the same for each inlet of that group.

When specifying the inlet group the following guidelines may be followed:

i. Since the **Inlet Group ID** is used to identify the inlets of the same inlet group, general information such as **Free Surface Level**, **Bottom Level**, or the mass flow rate for each phase should be the same for each inlet of the same inlet group.

ii. A different **Inlet Group ID** should be defined for each distinct inlet group. For example, consider the case of two inlet groups for a particular problem. The first inlet group consists of water and air entering through the same inlet (a single face zone). In this case, an inlet group ID of 1 should be specify for that inlet (or inlet group). The second inlet group consists of oil and air entering through the same inlet group, but each uses

a different inlet (oil-inlet and air-inlet) for each phase. In this case, the same **Inlet Group ID** of 2 should be specify for both of the inlets that belong to the inlet group.

Setting the Outlet Group: For pressure outlet or outlet vent boundaries, the **Outlet Group ID** is used to identify the different outlets that are part of the same outlet group. For instance, when phases enter through the same outlet (single face zone), then those phases are part of one outlet group and the **Outlet Group ID** should be set to 1 for that outlet (or outlet group). In the case where the same outlet group has separate outlets (different face zones) for each phase, then the **Outlet Group ID** will be the same for each outlet of that group.

When specifying the outlet group, the following guidelines may be followed:

i. Since the **Outlet Group ID** is used to identify the outlets of the same outlet group, general information such as **Free Surface Level** or **Bottom Level** should be the same for each outlet of the same outlet group.

ii. A different **Outlet Group ID** should be specified for each distinct outlet group. For example, consider the case of two outlet groups for a particular problem. The first inlet group consists of water and air exiting from the same outlet (a single face zone). In this case, an outlet number of 1 should be specify for that outlet (or outlet group). The second outlet group consists of oil and air exiting through the same outlet group, but each uses a different outlet (oil-outlet and air-outlet) for each phase. In this case, the same **Outlet Group ID** of 2 should be specify for both of the outlets that belong to the outlet group.

4.3 Validation

Validation is done by comparing the measured data from the site with simulated data. For this purpose, a well-defined, curved rectangular open channel of the 1X1000KW SHP station is chosen. This has been discussed in chapter-3; same measured velocity data is also used for validating the CFD solution procedure. These site conditions have been modeled and the flow is been simulated by CFD analysis. Comparison of these results is discussed in the following sections.

CFD analysis for this particular work is done in fluent software. In CFD, analysis prediction of the flow is done by solving the governing flow equations for each mesh. The exactness of this procedure with real data depends on the software used, size of the mesh used, and meshing scheme and the conditions specified in the solver. It is evident that the prediction may be prone to error. Therefore, closeness of these simulated profiles with the real situation has to be verified so that the accuracy of the simulated results can be trusted. But in rest of dissertation work CFD is used for modeling the trapezoidal open channel. Therefore it is important to know that final solution is also depends on meshing scheme used for modeling the geometry. For same boundary condition, the simulation solution may be different in simple rectangular and trapezoidal open channels. Because, for modeling the rectangular channel, hexahedral meshing scheme is applied, while in trapezoidal channel tetrahedral meshing scheme is applied. Therefore, in this work validation has been done for 45° bend rectangular channel for which modeling is done by tetrahedral type meshing scheme. So that trapezoidal channel simulation procedure is validated by 45°, bend rectangular channel simulation procedure.

4.3.1 Site Selection

Validation has been done in a 45 ° bend and well-defined geometry. The selected channel should be long enough to have a fully developed flow at the measuring section. An open-channel at 1x1000kw SHP in Punjab has been selected for measurements. It is a curved channel, with both sides wall vertical, 2.3 meters deep, 19.38 meters wide and radius of bend is 27 meters.

The conditions of the channel were very favorable to carry out a steady measurement with ADCP and PCM.

4.3.2 Modeling of Site in CFD

An exact model of the site with the above-mentioned geometry has been created and the meshing is done in Gambit as shown in Fig 4.2. For meshing the volume in Gambit, the following parameters should be specified:**1)** *Meshing Scheme* specified by 3 parameters (**Elements-** defines the shape of elements used to mesh the volume, **Type-** defines the meshing algorithms used and **Smoother-** describes the smoothing algorithm used, if any) **2)** *Mesh node spacing.*

Meshing Element used: tetrahedral– specifies that mesh include only tetrahedral elements.

Meshing Type used : tgrid- creates a regular structural grid of tetrahedral elements.

Mesh node spacing : 0.1 m. i.e. the whole volume will be divided into tetrahedral elements with face length equals to 0.1 m. The volume is initially checked with three different meshes spacing of 0.3 m, 0.2 m and 0.1 m and the improvement in the simulation results was observed as the grid size reduces. However, number nodes that could be import in FLUENT are limited to maximum 10, 00000. Therefore, mesh spacing is selected to be 0.175 m in this work and 0.1m for rest of the dissertation work

After meshing the volume, grid check has been conducted to ensure the regularity of the cells formed. The meshing is considered good if volume passes grid check.

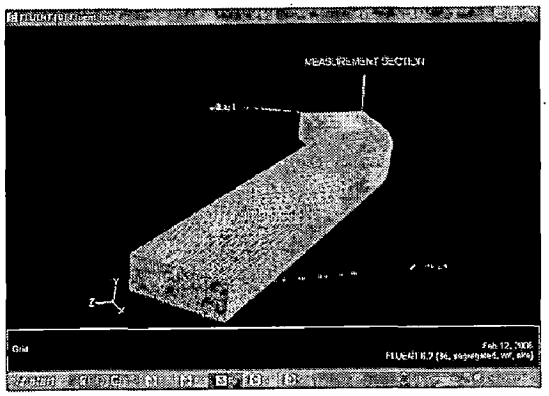

Fig 4.2 Rectangular open channel with 45° for validation modeled in Gambit

Specifying zone types: Zone-type specifications define the physical and operational characteristics of the model at its boundaries and within specific regions of its domain. There are two classes of zone-type specifications:

i. Boundary types – WALL type for side walls and bed, VELOCITY INLET for inflow, MASSFLOW_INLET for free surface, OUTLET VENT for outlet
ii. Continuum types – FLUID, whose specifications define the physical characteristics of the model within specified regions of its domain. Here it is water flow.

4.3.3 Profile Simulation in CFD

The open channel flow is modeled by initializing boundary condition that is discussed systematically in following section with the help of fluent GUI sub window.

Step-1: firstly case file of meshed geometry is read. Three general multi phase models are available, such as Volume of Fluid (VOF), Eulerian and Mixture models as shown in Fig 4.3. The VOF model is appropriate for stratified or free-surface flows, and the mixture and Eulerian models are appropriate for flows in which the phases mix or separate. The solver used is the segregated solver. In this solution algorithm, the governing equations are solved sequentially.

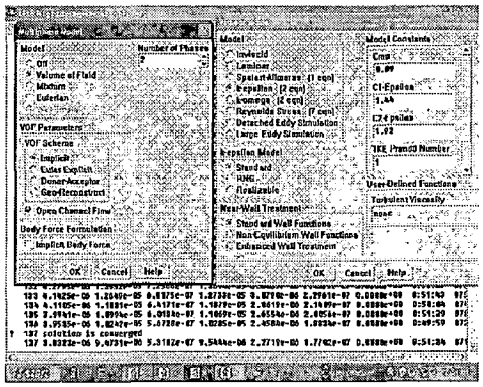

Fig 4.3 Multiphase and viscous sub-menu of FLUENT

Step-2: As shown in Fig 4.4, the flowing fluid martial type have to be selected from fluent materials database and selected the water-liquid as fluid type. Then clicked the change create icon to define the water properties and clicked copy icon for initialization of water properties.

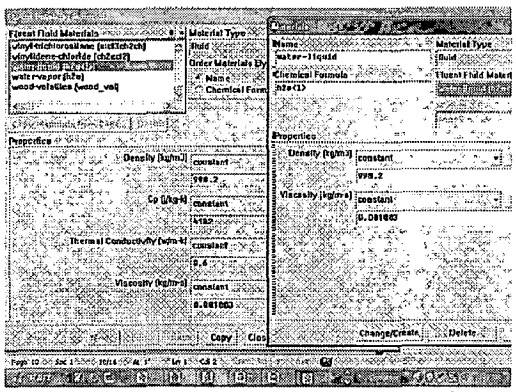

Fig 4.4 Materials database sub menu of FLUENT

Step-3: The operating conditions have to be specified such as the direction of flow, the direction of gravity and the density of lightest phase, i.e. air. The lightest phase air is set as primary phase and water as secondary phase in open channel flows as shown in Fig 4.5.

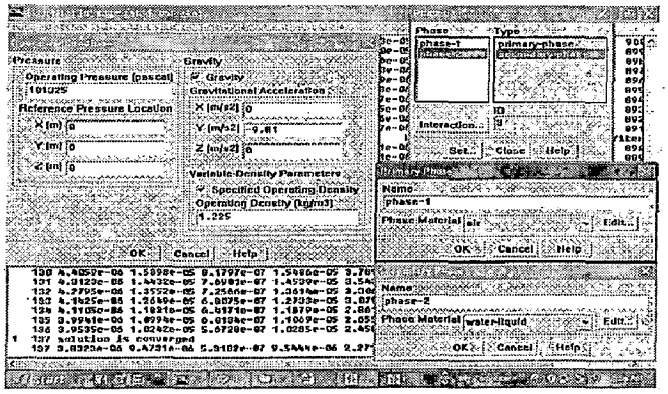

Fig 4.5 Operating condition and phases sub menu of FLUENT

Step 4: Velocity inlet boundary condition is defined with inlet velocity equal to 1.185 m/s with the flow direction in x-axis, and turbulence condition defined as shown in Fig 4.6

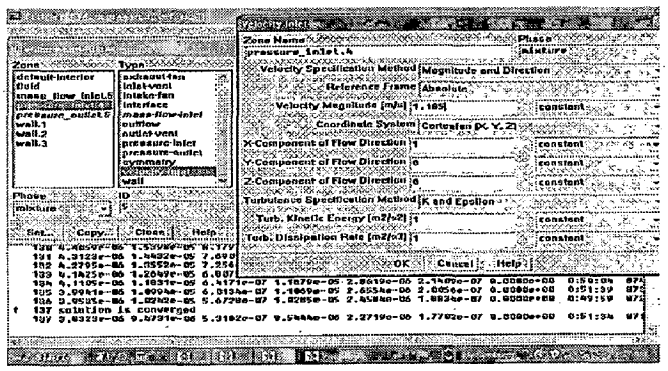

Fig 4.6 Inlet boundary condition sub menu of FLUENT

Step 5: MASS FLOW INLET should be applied for compressible flow. As shown in Fig 4.7. It is defined as a free surface condition and open channel inlet option is selected for defining the free surface and bottom level of the water.

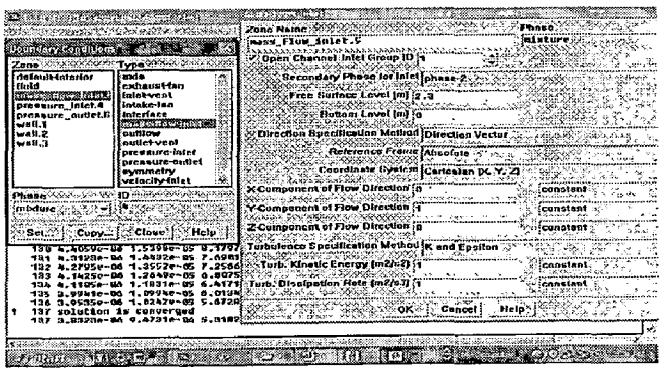

Fig 4.7 Mass flow inlet condition sub menu of FLUENT

Step-6: OUTLET VENT is defined as outlet boundary condition and open channel is selected for defining the free surface and bottom level at outlet as shown in Fig 4.8 Where bottom level is defined by considering the bed slope that is given 0.0002m/1m according to Manning's Formula, which is given below in equation 4.3.

$$V = \frac{1}{n} R^{2/3} S_0^{1/2} \tag{4.3}$$

where,

V is flow velocity in the channel, in m/s.

n is a roughness coefficient.

R is hydraulic radius of a channel, in m.

S_0 is a bed slope, in m/m.

The value of roughness coefficient varies according to nature of boundary surface. In this work, Value of n is chosen from 0.011 to 0.019.

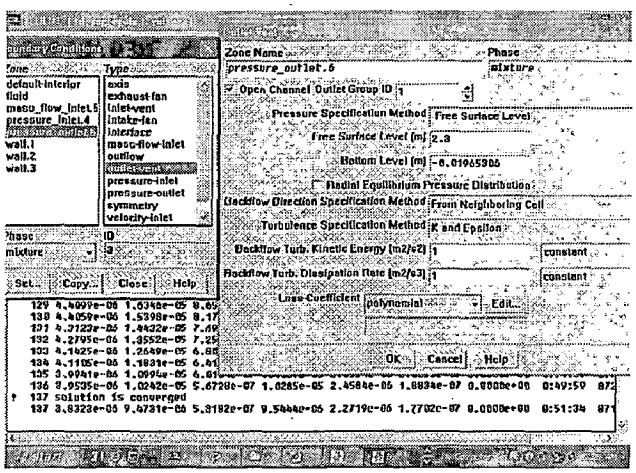

Fig 4.8 Outlet boundary condition sub menu of FLUENT

Step 7: Once boundary condition is defined. In next step, convergence criteria are defined as shown in Fig 4.9(a). Finally FLUENT will calculate the initialization condition when inlet velocity is selected for initializing the solution. Solution is iterated by initializing 1000 iteration. Number of iteration is required to converge the solution, which depends on residual condition. As residual value decreases, number of iteration to converge the solution increases. For this validation work, 0.00001 residual values are defined and solution is converged with 137 iterations as shown in Fig 4.9. Accuracy of final solution is increase as decrease the residual value. For this

validation work, the residual plot of all components is shown in Fig 4.9(b). All components are plotted with different colors, when its value decrease beyond convergence criteria then solution will converge.

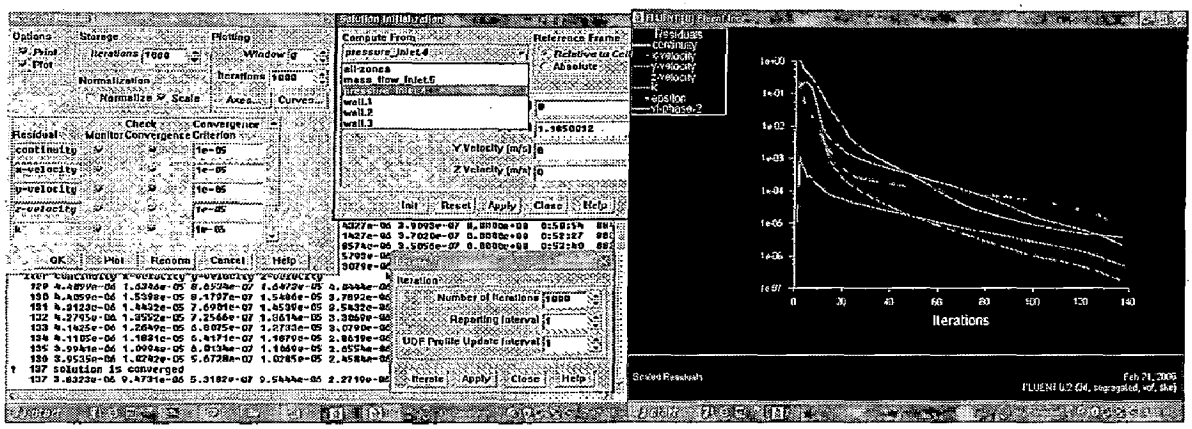

Fig 4.9 (a) Residual monitoring sub menu (b) Residual plot after convergence of solution

Step 8: After solution is conversed, velocity contour at various surface can be examined by selecting the contours option in display Menu and defined the contours sub window as shown in Fig 4.10. Simulated velocity contour of a rectangular open channel with 45° bend is shown in Fig 4.11. Matrix of velocity data at any surface can be read from write profile sub window in DEFINE main menu in FLUENT GUI as shown in Fig 4.10. Simulated data can be read by EXCEL sheet. Here in this work this velocity data is used for calculating the average velocity at that surface and compared it with real measured data for validating the CFD solution procedure.

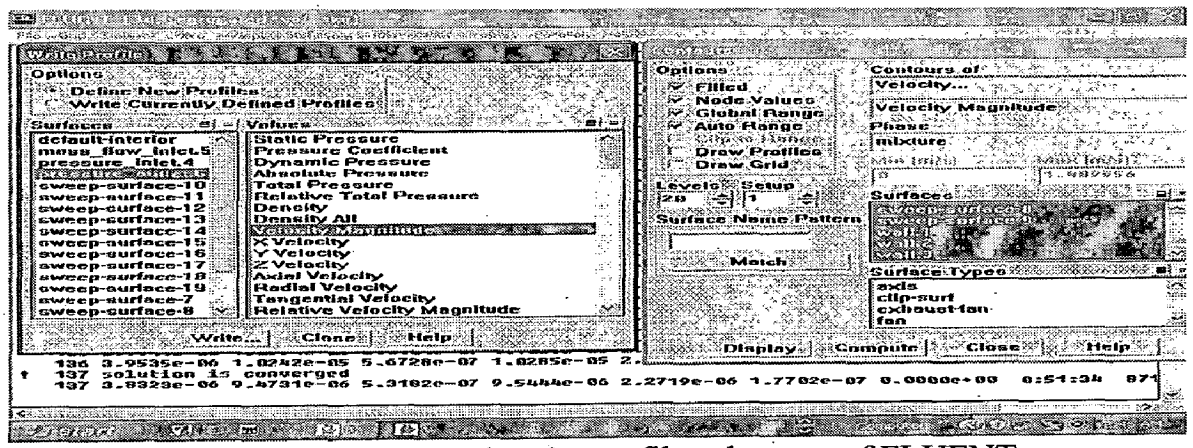

Fig 4.10 Contours and Write profile sub menu of FLUENT

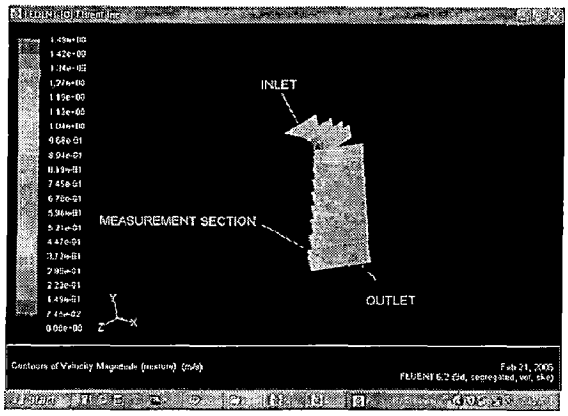

Fig. 4.11 Simulation of flow in CFD

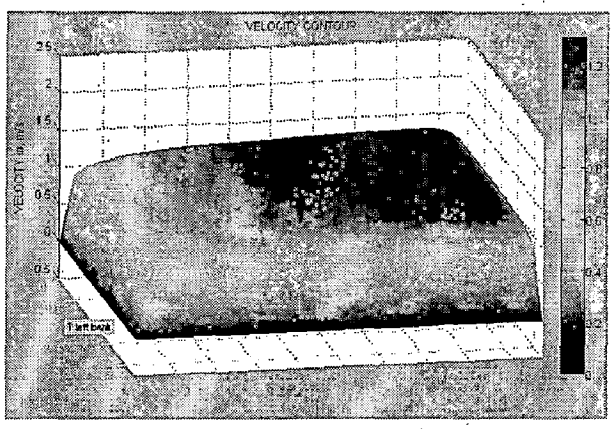

Fig. 4.12 3-D velocity profile plot of simulated data

In this work, MAT LAB coding is done for creating 3D velocity contour of simulated data as shown in Fig. (Fig 4.12), it is evident that flow is more in right region of measurement section.

The flow rate measurement at site is done using ADCP and PCM as discussed in chapter-3. Those measured velocity data are used for developing 3D velocity contour as shown in Fig 4.13. Small picks in 3D profile of PCM data at middle and nearer to sidewalls shows variation in PCM data. 3D profile of H-ADCP data is uniform as shown in Fig 4.13(a).

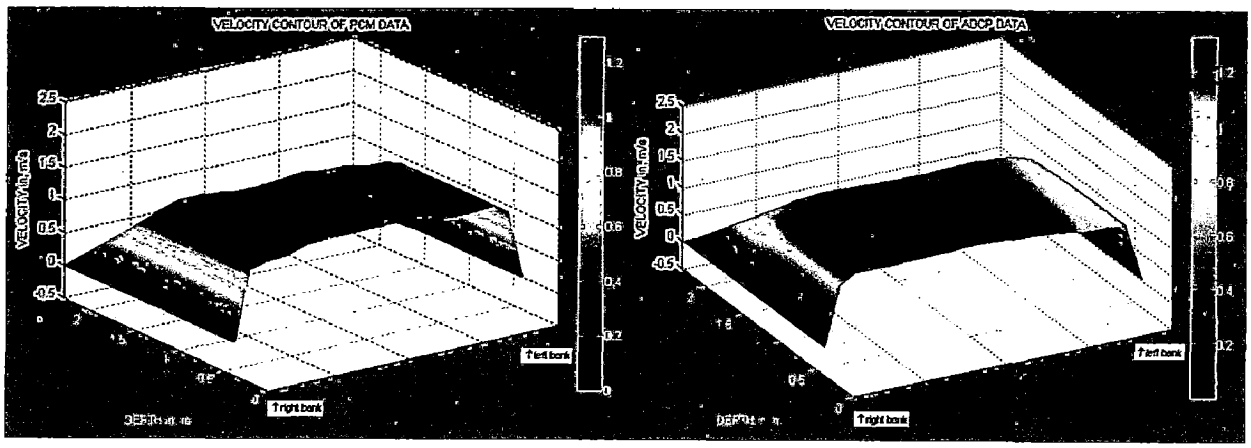

Fig. 4.13 3D profile for (a) PCM and (b) ADCP data

4.4 Results of Validation

Validation is done by comparing the simulation result and the site data. The average velocity vs. depth and partial discharge vs. width profile is compared for both measured and simulated data. Total Discharge in the channel is computed from velocity data by using velocity area integration method as discussed in chapter 3. Average velocity and discharge reading of simulated and measured data is given in Table 4.2.

Table 4.2 Result of simulated and measured data

	CFD result	ADCP	PCM
Average velocity m/s	1.1858504	1.18360793	1.1953399
Discharge m^3/s	52.85810830	52.7581083	53.281083

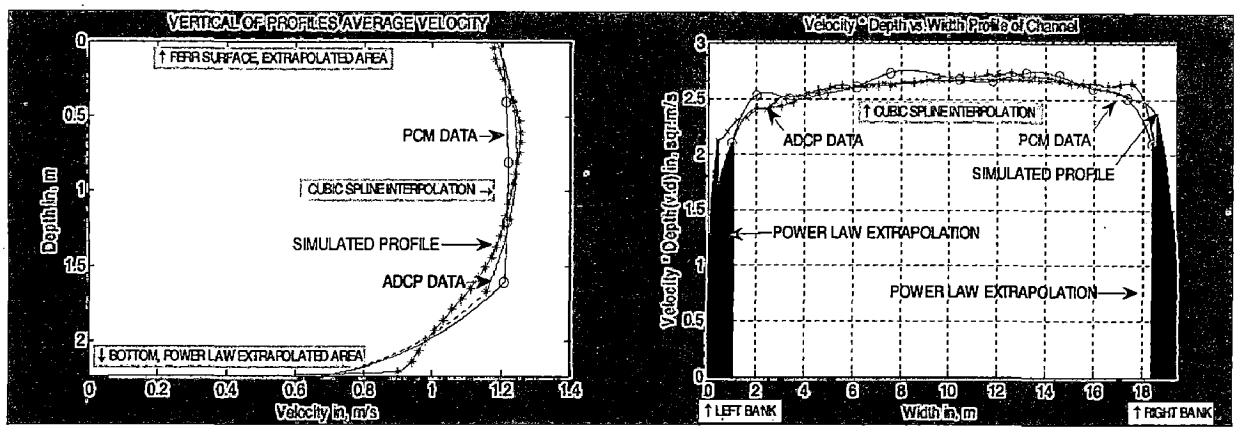

Fig 4.14 Comparison of (a) average velocity vs. depth (b) partial discharge vs. width profiles

Observations:

i. The velocity vs. depth profile of simulated data and measured data by ADCP and PCM is found to be almost same.

ii. The discharge evaluated for the three data is only varying by less than 1%. This variation in magnitude and slight difference of the two profiles may be due to the approximation of average velocity at inlet in CFD simulation and due to discretization in CFD procedure. The measurement errors of the real data and discharge computational methodology may also contribute for this slight discrepancy.

iii. Horizontal and vertical profile of the ADCP data is more coinciding with CFD data as compared to PCM data. this variation in PCM data due to several factors that has been mentioned in chapter-3

In spite of this slight variation in magnitude the profiles is observed to be almost identical, means the CFD simulations can rely upon further open channel analysis.

4.5 Effect of Aspect Ratio on Velocity Profile

Flow in open channel strongly depends on the aspect ratio $X = {}^{w}/_{d}$, where w is the channel width and d is the flow depth. According to this ratio, open channel can be classified as narrow or wide such as[19]:

i. Narrow channel ($X \leq 5$): Secondary flow due to sidewall effects result in a dip in the velocity distribution near the surface such that the maximum velocity is below the water surface.

ii. Wide channel ($X > a = 5$): The strength of secondary flow velocity due to sidewall effects is reduced in the central zone of the channel with a band of width equal to $w - a * d$. Maximum velocity is found at free surface.

The vertical distribution of velocity in open channel is very complex. Juan A Gonjalez [19] identified three regions in the vertical flow field for steady uniform flow in smooth, wide open channels; "(1) The wall region, [y/d ≤ 0.15 to 0.2, y is the distance above the bottom wall], referred as the inner layer in boundary layer theory, where length

and velocity scales are v/u* and u_* , where v is the kinematics viscosity of the fluid, u_* is the boundary shear velocity defined as $u_* = \sqrt{\tau_b / \rho}$, τ_b is boundary shear stress, and ρ is the fluid density; (2) The free surface region, [0.6≤d/D≤1], where the length and velocity scales are the flow depth D and the maximum velocity u_{max}; and (3) The intermediate region 0.15 to 0.2<d/D<0.6, That is not strongly effected by either the wall properties or the free surface".

The distribution of velocity in a fully developed open channel is dependent on the geometry of the channel. In wide-open channel, the velocity is zero at solid boundaries and gradually increases with distance from the boundary. The maximum velocity in a vertical of the cross-section occurs at a free surface. There is no dip phenomenon in the central region; therefore, average velocity profile can be mimic by logarithmic or power law distribution up to free surface. In this work, average velocity profile of simulated data is compared with logarithmic, power law, logarithmic plus parabolic and power law plus parabolic profiles. The logarithmic equation is given as in equation 4.4[19, 20]

$$\frac{V_d}{\mu_*} = \frac{1}{\kappa} \ln\left(\frac{d}{k_s}\right) + A \qquad (4.4)$$

Where,

k =is kalman constant, equal to 0.41.

A =is constant

V_d =is velocity at depth d from bottom.

μ_* =is boundary shear velocity.

Several methods are available to estimate μ_* the simplest one derived [19] for steady uniform flow in open channels as $\mu_* = \sqrt{sgD}$ where, s is the slope of channel bed, g is gravitational force, D is total depth of water in the open channel the roughness of the channel is represented by Nikurade's equivalent k_s, which accounts for the effect of the roughness elements. The roughness in the open channel can be classified according to ratio of roughness and viscous length scales $k_s^+ = \frac{\mu_* k_s}{\nu}$ such as:

Smooth channel	$k_s^+ < 5$
Transitional rough channel	$5 < k_s^+ < 70$
Fully rough channel	$k_s^+ > 70$

In this work, the solid boundaries considered as concrete type so that roughness is between 5 and 70 that has been determined for various geometry [19, 21]. Logarithmic law is inherently valid only in wall region. Power law can be also used to represent the vertical velocity distribution in fully developed sub critical open channel flow through smooth channel, can be represented by equation (4.5) [19]:

$$\frac{V}{\mu_*} = C*\left(\frac{d*30}{k_s}\right)^{1/m} + a \tag{4.5}$$

Where C is a constant, and is equal to 8.3 according to schlichting's boundary layer theory (1979) [22]. m is power law exponent constant that vary from 2 to 10, for completely rough channel m=2 and for smooth channel m=10.

For narrow open channel the maximum velocity is at some distant below the free surface, dip phenomenon occurs. So that power law and logarithmic law cannot be extended to the free surface, therefore the outer region is modeled by the parabolic low, have been mentioned in reference [23]. Parabolic law equation is given in equation 4.6[23]. In this work, Coefficient has been determined for rectangular open channels.

$$\frac{V_d}{\mu_*} = \mu_{\max} - \left(B*\left(1-\left(D-d\right)-d\right)\right)^2 \tag{4.6}$$

where,

$\mu_{\max}$ is maximum velocity in the channel

B is constant, equal to 9.6.

D is depth at which velocity being determined

Above parabolic equation can be applied for sub critical smooth rectangular narrow open channels. Logarithmic or power law plus parabolic law are used to mimic vertical velocity distribution in narrow channel, its coefficient is determined for simulated

channel that is presented in next section of this chapter. Focus of this section is to study the effect of aspect ratio by CFD simulation and compared with the above theoretical concept by implementing the above equation in MAT LAB.

4.5.1 Rectangular Narrow Channel (Geometry –1)

Here, the variation in the velocity profile of simple rectangular narrow channel is studied by modeling the geometry and simulating the flow. An OUTLET plane is selected as the measuring section and velocity profile developed in the measuring section is analyzed. Geometry is meshed in GAMBIT as shown in Fig 4.15

Site specifications:

Depth=2m, Width=3m, Length = 20m, Slope = 0.00022 m / 1m

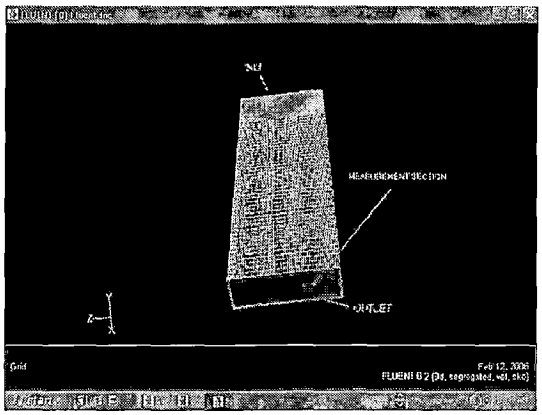

Fig. 4.15 Rectangular narrow channel

(I) Profile Simulation In CFD

The convergence criteria are specified same as defined in validation section. Except the average velocity magnitude in inlet, this is given as 0.8 m/s and hexahedral type meshing scheme is selected for meshing the simple rectangular channel. After the parameters are set, the solver is initialized with inlet conditions and the iteration is done. 200 iterations were given inside which the solution has converged. The simulation result of the flow in the channel is shown in Fig. 4.16. 3D and 2D velocity contour is developed from simulated matrix of data as shown in Fig 4.17. It is observed the maximum velocity at below the free surface [24].

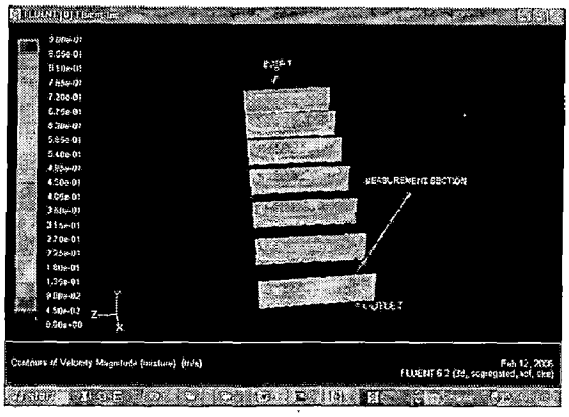

Fig 4.16 Velocity contour of a rectangular narrow channel (Simulated in CFD)

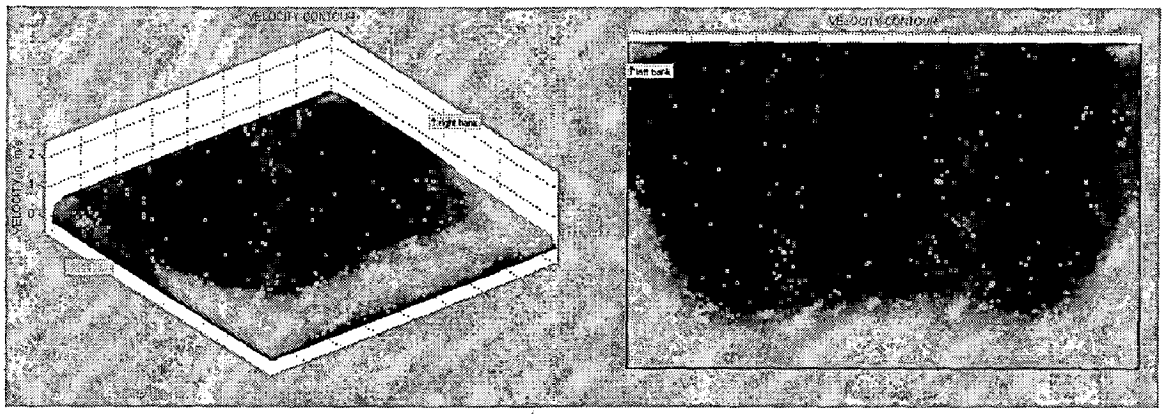

Fig. 4.17 (a) 3D velocity contour and (b) 2D velocity contour of simulated data

(II) Comparison Of Simulated And Theoretical Profile

As discussed above, in rectangular narrow open channel, maximum velocity is observed below the free surface. Velocity vs. depth profile is created from simulated data and compared with vertical profiles that are mimicked, by logarithmic and power law at inner zone and parabolic law at outer zone, from free surface to up to 0.15 of the flow depth, vertical profile is developed by implementing above three fundamental equations in MAT LAB. Comparison of simulated and theoretical profile is shown below in Fig 4.18. Appropriate values of coefficient of above three equations are selected for modeling the flow and are given in the Table 6.5.

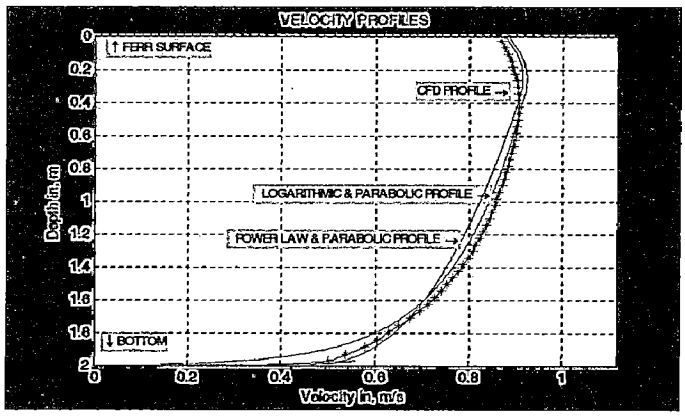

Fig 4.18 Comparison of vertical profile of simulate and theoretical data

Table 4.3 Parameter of mathematical equations

Boundary shear velocity u_*	0.0638
Viscosity v	61408
Coefficient- A	3.57
Roughness constant K_s	65
Power law exponent m	2.5
Coefficient a	0.435

(III) Comparison Of Average Velocity Computation Methods

Inlet velocity in CFD is taken as a true value for analyzing accuracy of average velocity computational methods. Comparison of reduce point averaging methods is given in Table 4.4.

Table 4.4 Comparison of reduce point averaging methods

Reduce Point Averaging Method	Average velocity, m/s	% error
1 point at (0.6 * d)	0.853459	6.682481
1 point at (0.625 *d)	0.855676	6.959562
2 points	0.812321	1.540136
3 points	0.816793	2.099139
3 points weighted	0.825679	3.209885
4 points	0.821807	2.725900
5 points	0.818032	2.254041
6 points	0.821516	2.689601

(IV) Result And Discussion

i. Two point averaging method is accurate as compared to other reduce point averaging methods.

ii. One-point gives large error; therefore, it should not be used for computing the average velocity in the simple rectangular narrow channel.

iii. The theoretical profile showed excellent coincidence with simulated profile

iv. Average velocity values- logarithmic and parabolic profile=0.801326
Power law and parabolic profile=0.801901

4.5.2 Rectangular Wide Channel (Geometry –2)

Here, the variation in the velocity profile of simple rectangular wide channel is studied by modeling the geometry and simulating the flow. An OUTLET plane is selected as the measuring section and velocity profile developed in the measuring section is analyzed. Geometry is modeled in GAMBIT as shown in Fig 4.19

Site specifications:

Depth = 2.3m, Width= 19.38m, Length = 100m, Slope = 0.00022 m / 1m

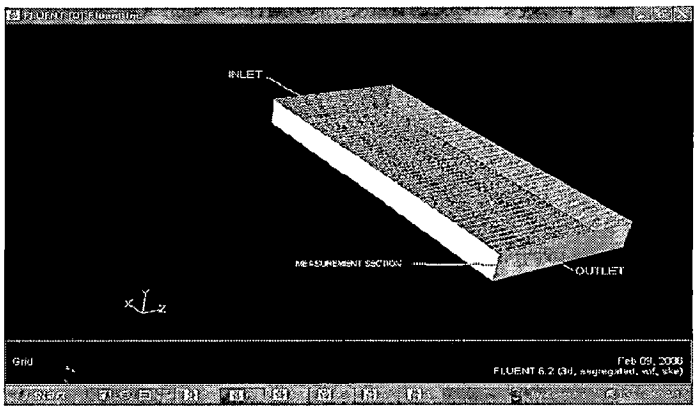

Fig. 4.19 Rectangular wide open channel

(I) Profile Simulation In CFD

The convergence criteria are specified same as defined in validation section. Except the average velocity magnitude in inlet, this is given as 1.5 m/s and hexahedral type meshing scheme is selected for meshing the simple rectangular channel. After the parameters are set, the solver is initialized with inlet conditions and the iteration is done. 200 iterations were given inside which the solution has converged. The simulation result

of the flow in the channel is shown in Fig.4.20. 3D and 2D velocity contour is developed from simulated matrix of data as shown in Fig 4.21.

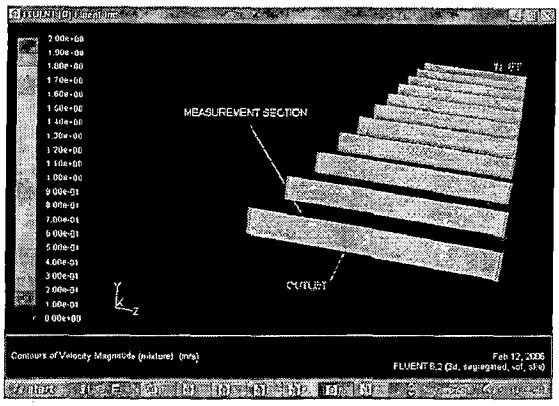

Fig 4.20 Velocity contour of a rectangular wide channel (Simulated in CFD)

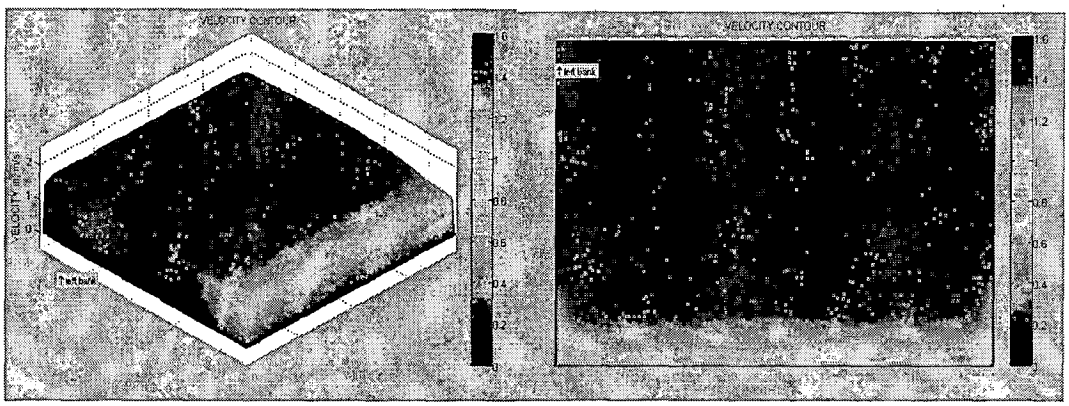

Fig.4.21 (a) 3D velocity contour and (b) 2D velocity contour of simulated data

(II) Comparison Of Simulated And Theoretical Profile

As discussed above, in rectangular wide-open channel maximum velocity is observed at the free surface. Velocity vs. depth profile is created from simulated data and compared with vertical profiles that are created by logarithmic and power law shown in Fig 4.21. In addition, it is compared with vertical profiles that are created by logarithmic and power law at inner zone and parabolic law at outer zone from free surface to up to 0.15 of the flow depth, vertical profiles is developed by implementing above three fundamental equations in MATLAB. Appropriate values of coefficient of above three equations are selected for modeling the flow that is given in the Table 4.5. For transitional rough channel (concrete structure), power law exponent m is equal to 3.5.

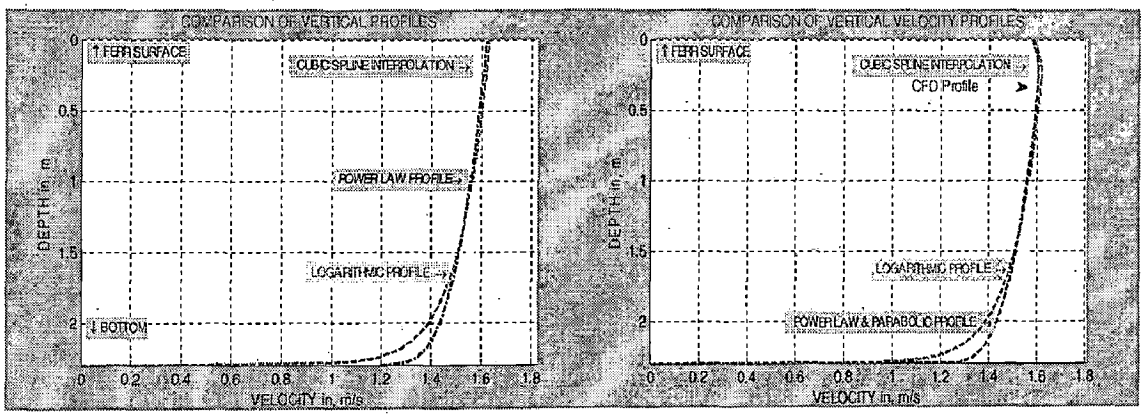

Fig 4.22 Comparison of vertical profile of simulated and theoretical data of (a) logarithmic and power law (b) logarithmic and power law plus parabolic

Table 4.5 Parameter of mathematical equations

Boundary shear velocity u_*	0.05
Viscosity v	61408
Coefficient- A	3.7
Roughness constant K_s	65
Power law exponent m	3.5
Coefficient a	1.2

(III) Comparison Of Average Velocity Computation Methods

Inlet velocity is taken as a true value for analyzing accuracy of average velocity computational methods. Comparison of reduce point averaging methods is given in Table 4.6.

Table 4.6 Comparison of reduce point averaging methods

Reduce Point Averaging Method	Average velocity, m/s	% error
1 point at (0.6 * d)	1.594003	6.266886
1 point at (0.625 *d)	1.594990	6.332691
2 points	1.528198	1.879922
3 points	1.550133	3.342244
3 points weighted	1.561101	4.073404
4 points	1.555398	3.693201
5 points	1.520521	1.368110
6 points	1.528627	1.901857

(IV) Results And Discussion

i. Five point averaging method is accurate as compare to other reduce point averaging method.

ii. One-point methods are giving large error; therefore, it should not be used for computing the average velocity in the simple rectangular wide channel.

iii. It is observed the logarithmic plus parabolic, and power law plus parabolic profiles showed excellent coincidence with simulated profile as compared to logarithmic and power law profiles, as shown in Fig 4.22.

iv. Average velocity values- logarithmic profile=1.516354 m/s
Power law profile=1.560443 m/s
Logarithmic and parabolic profile=1.51394 m/s
Power law and parabolic profile=1.53105 m/s

Data of averaging methods are further used for overall comparison of averaging methods in chapter 5.

CHAPTER 5

TRAPEZOIDAL CHANNEL FLOW SIMULATION

The discharge measurement with desired accuracy can be done in simple straight rectangular open channel. However, desired situation may not be always present at field measurement site especially in small hydro power plants. If a measurement has to be done in undesirable conditions such as trapezoidal channel with bending, divergence, and convergence, this may lead to large measurement errors. The irregularity of the open channel is one of the major factors, which add to the measurement uncertainty. The velocity profiles developed in various open channel geometries is found to be very complex, that the accurate measurement of these profiles is a tedious and challenging job.

In this work, an effort has been made to investigate the velocity profiles of various trapezoidal and semi-trapezoidal open channels and to analyze the accuracy of average velocity computational methods, and developed methodology for discharge computation in trapezoidal open channel. The effect of power law extrapolation and cubic spline interpolation in discharge measurement by using width velocity integration method is analyzed in six different open channels. CFD analysis is used for simulating the flow in six different geometries and the results are discussed in this chapter. Analysis of two rectangular channels has been discussed in chapter 4. All the geometries are modeled with similar operating and boundary conditions, same as that used for the validation site. Therefore, these conditions are not repetitively mentioned here.

5.1 Discharge Computation Method for Trapezoidal Channel

The discharge computation method for rectangular open channel is standardized by ISO-748. That has discussed in chapter 3. Same method can be applied for trapezoidal channel. However, few number of velocity data that could be measured in a vertical at trapezoidal section of trapezoidal channel. Therefore, interpolation and extrapolation may not be accurately predicting the velocity distribution in unmeasured zone. Methodology for discharge computation is developed by considering principle of H-ADCP. As

discussed in chapter 3, H-ADCP scans velocity at each cell in a horizontal section. Therefore, cubic spline interpolation and extrapolation of large number of measured data can be accurately carried out. As shown in Fig 5.1, Discharge is computed in two-step, (1) Partial discharge at a level of measurement section is determined by integrating the velocity over a width of the channel instead of integrating velocity over the depth of the channel. (2)Finally, discharge is computed by integrating the partial discharge over depth of the channel. The velocity and partial discharge between measured velocity points and between computed partial discharge points is estimated by cubic spline interpolation. Velocity and partial discharge at periphery of the channel is estimated by power low extrapolation or by cubic spline extrapolation. In the rest of the work, this method is used for computing the discharge in the channel. The discharge computation methodology is implemented in MATLAB.

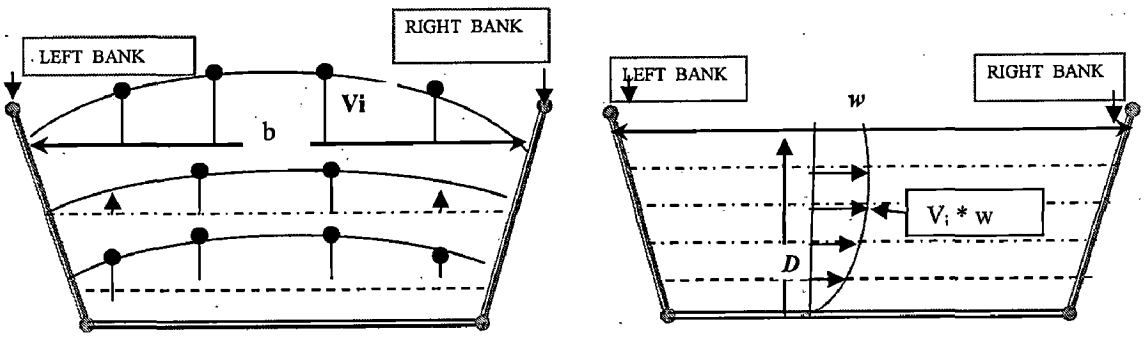

Fig 5.1 (a) Width vs. Velocity horizontal (b) Velocity * Width vs. Depth profile.

5.2 Straight Trapezoidal Open Channel (Geometry –3)

An open channel trapezoidal geometry with sloped sidewalls and very small bed slope is developed and the meshing is done in Gambit as shown in Fig 5.2. Where slope of the bed is chosen according to mannig's rule that is discussed in chapter 4. The details of site modeling- meshing schemes used and mesh node spacing is similar as that for the site model discussed in validation process, the details of which is given in section 4.3. The developed model is straight enough to produce a fully developed flow. In CFD modeling, unlike the real situation the conditions are set to be ideal to produce a steady flow.

Channel dimension:

Depth = 2m, Width at Bottom= 3m, Width at Surface=7, Length = 35m,

Slope= 0.0022 m / 1m, Side slope= 2m /2m

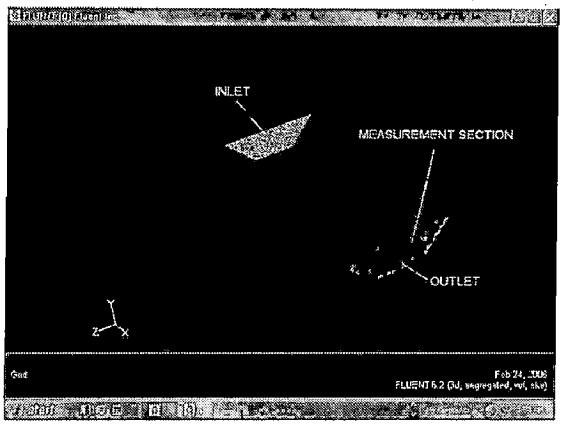

Fig.5.2 Trapezoidal channel modeled in Gambit

5.2.1 Profile Simulation in CFD

Open channel modeling is done by using multi phase VOF model. The boundary types are specified such as VELOCITY INLET for inlet, MASS FLOW INLET for free surface, OUTLET_VENT for outlet, WALL for sidewalls and bed. The boundary parameters are same as that discussed for validation site, except for the average velocity magnitude in inlet, which is given as 0.3 m/s. After the parameters are set, the solver is initialized with inlet conditions and the iteration is done. 200 iterations where given inside which the solution has converged. The simulation result of the flow in the channel is shown in Fig 5.3. It is observed the maximum velocity at middle of measurement cross-section. The velocity vs. width and partial discharge vs. depth profile are created from simulated matrix of data and it is observed the power extrapolation with m=three gives smooth profile as shown in Fig 5.4.

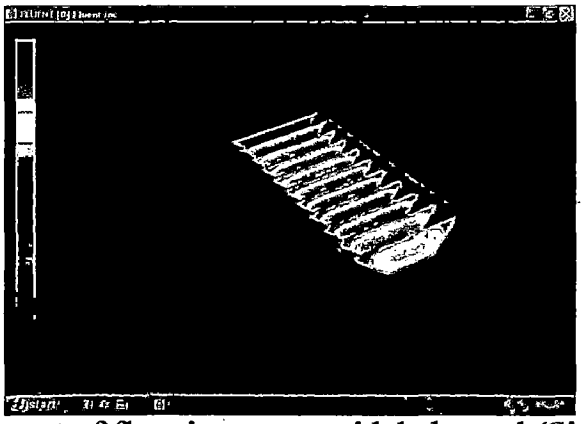

Fig 5.3 Development of flow in a trapezoidal channel (Simulated in CFD)

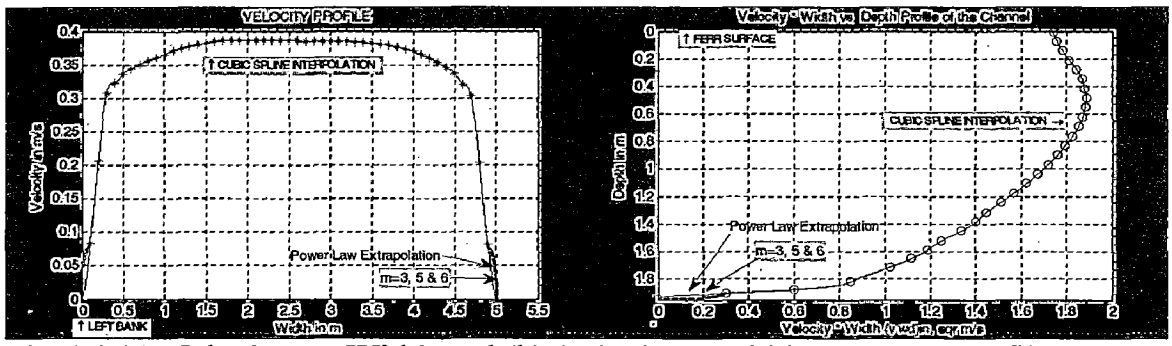

Fig.5.4 (a) Velocity vs. Width and (b) Velocity * Width vs. Depth profile of simulated data

5.2.2 Comparison of Average Velocity Computation Methods

The discharge in the channel is computed according to methodology discussed in section 5.1. The discharge in the channel is always constant. Therefore, average velocity in an open channel is also constant for fully developed uniform steady flow. Therefore, inlet velocity is taken as a true value for computing the error in average velocity computational methods. The convergence criteria are also taken same as defined in validation section. Averaging methods has discussed in chapter 1. Two integration methods are used for computing the average velocity at a level. (1) By cubic spline interpolation of measured data and zero velocity that is considered at solid boundary of the channel. (2) By interpolating the measured data and by power law extrapolation of first and last measured velocity point to solid boundary. Comparison of averaging methods is given in Table 5.1.

Table 5.1 Comparison of averaging methods in geometry -3

Averaging Method	Computation Method	Average velocity, m/s	% error
Reduce point Averaging methods	1 point at (0.6 * d)	0.327800	9.266736
	1 point at (0.625 *d)	0.327174	9.058312
	2 points	0.305577	1.859106
	3 points	0.315557	5.185921
	3 points weighted	0.320547	6.849326
	4 points	0.317612	5.870852
	5 points	0.307534	2.511426
	6 points	0.310274	3.424668
Integration method (CSI)	4 Level integration	0.291761	-2.74607
	5 Level integration	0.297442	-0.85190
	6 Level integration	0.299919	-0.02669
	8 Level integration	0.297663	-0.77869
Integration method (Power law Extrapolation & CSI)	4 Level power law	0.301407	0.469279
	5 Level power law	0.300949	0.316610
	6 Level power law	0.300130	0.043498
	8 Level power law	0.297733	-0.755401

5.2.2 Results and Discussion

Velocity distribution in trapezoidal open channel is different from the rectangular channel. 3D and 2D velocity contour of measurement section is created from measured data as shown in Fig 5.5. Maximum and lowest velocity is observed in middle section and at solid boundary respectively.

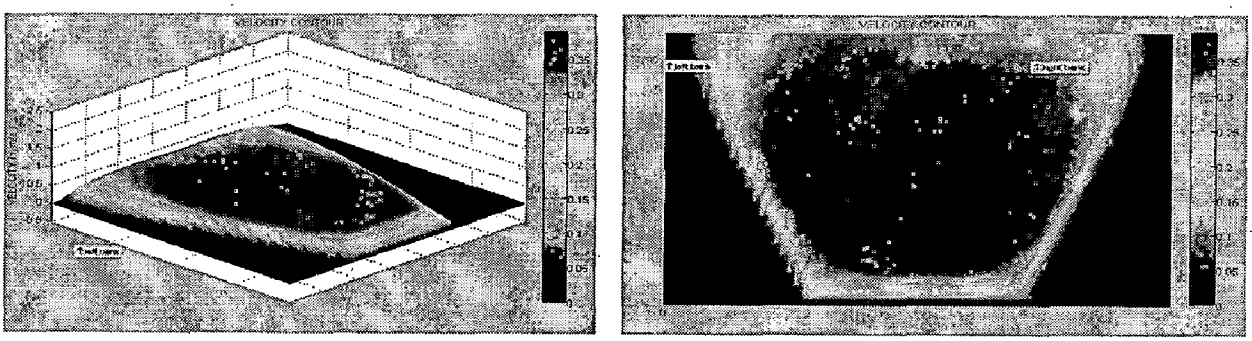

Fig 5.5 (a) 3D and (b) 2D velocity contour of simulated data

i. Two point averaging method is accurate as compare to other reduce point averaging methods.

ii. One-point and three point methods is give large error. Therefore, it should not be used for computing the average velocity in the simple straight trapezoidal channel.

iii. As shown in Fig 5.6, the cubic spline interpolation is failed to mimic the actual partial discharge vs. depth profile of four levels method. Therefore, CSI integration method should not be used in less than five levels method. Power law extrapolation with m=three should be used in more than four number of levels for computing the discharge in the channel.

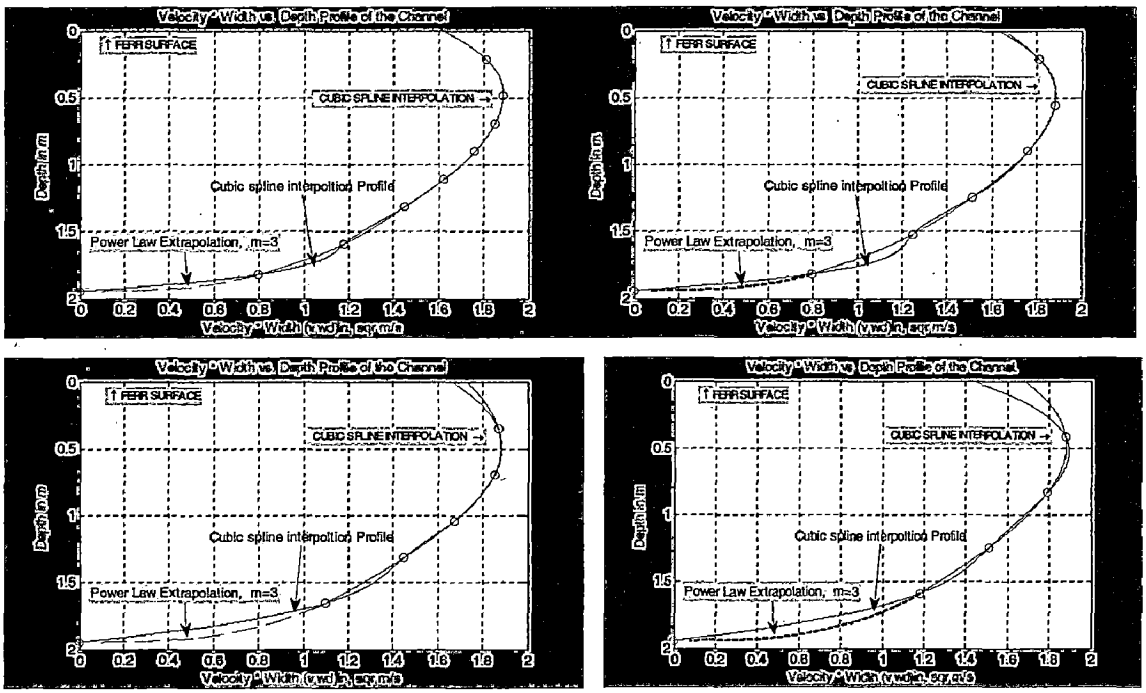

Fig 5.6 Comparison of vertical profiles of (a) 8 levels (b) 6 levels (c) 5 levels (d) 4 levels integration methods

iv. Average velocity is computed by average width method (considering the trapezoidal channel as rectangle channel), as shown in Table 5.2. It is observed that, if width of trapezoidal section of trapezoidal channel is increase, the accuracy of average width method is decrease.

v. Extrapolation is also required for computing the discharge from simulated data. The effect of power law exponent m in discharge computation is given in Table 5.2. Accuracy is improved as power law exponent is decreased. So that

to improve the accuracy of discharge computation, value of m should be used between two to four.

Table 5.2 Comparison of integration method with m=3, 5 and 6 (geometry -3)

Method	Average Velocity, m/s	% error
True value	0.3	---
Average width method	0.305904	1.968333
Integration method (Power law Extrapolation & CSI) with m=3	0.301974	0.658244
Integration method (Power law Extrapolation & CSI) with m=5	0.302471	0.823959
Integration method (Power law Extrapolation & CSI) with m=6	0.302613	0.871294

5.3 Trapezoidal Channel with 90° Bend (Geometry –4)

Bend in the channel is one of the major factors, which affect the velocity profile. Here the variation in the velocity profile caused due to a 90° bend is studied by modeling the geometry and simulating the flow. An OUTLET plane is selected as the measuring section and velocity profile developed in the measuring section is analyzed. Geometry is meshed in GAMBIT as shown in Fig 5.7

Channel dimension:

Depth = 2m, Width at Bottom= 2m, Width at Surface=6, Length= 30m,

Slope= 0.00022 m / 1m, Side slope= 2m /2m, Bend 90°

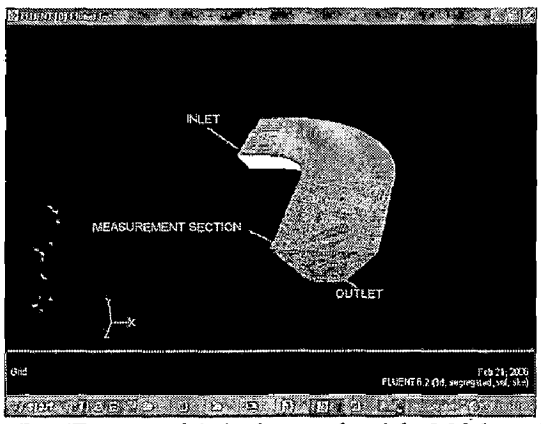

Fig.5.7 Trapezoidal channel with 90° bend

5.3.1 Profile Simulation in CFD

The convergence criteria are defined same as given in simple straight trapezoidal channel. Except the average velocity magnitude in inlet, this is given as 0.5 m/s. After the parameters are set, the solver is initialized with inlet conditions and the iteration is done.

200 iterations where given inside which the solution has converged. The simulation result of the flow in the channel is shown in Fig 5.8. It is observed the maximum velocity at right side of the channel. The velocity vs. width and partial discharge vs. depth profile is created from simulated matrix of data as shown in Fig 5.9. Maximum partial discharge is observed below the free surface as shown in Fig 5.9(b). Here the flow is set to x-direction in the inlet and z-direction in the outlet (to account for 90° bend).

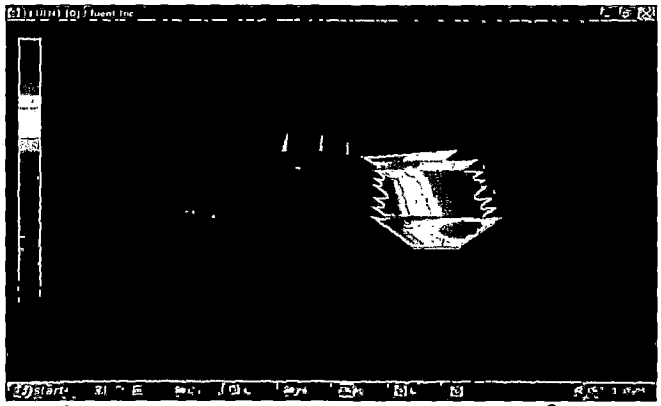

Fig 5.8 Development of flow in a trapezoidal channel with 90° bend (Simulated in CFD)

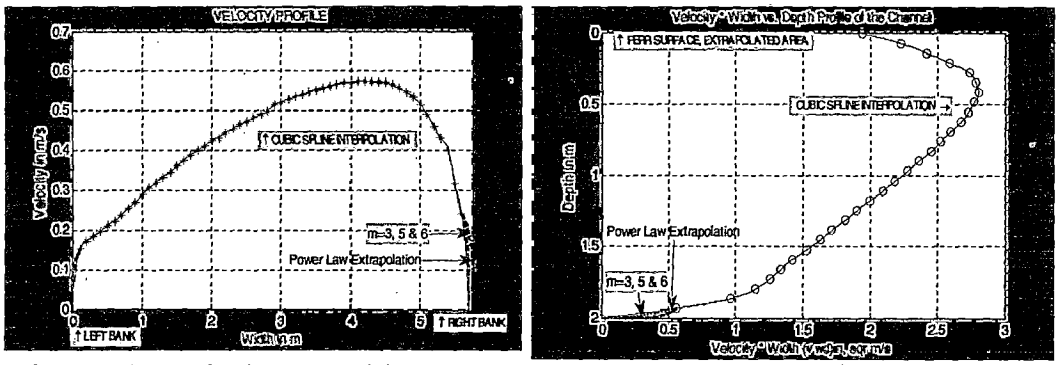

Fig. 5.9 (a) Velocity vs. Width and (b) Velocity * Width vs. Depth profile of simulated data

5.3.2 Comparison of Average Velocity Computation Methods

As discussed in section 5.2. Inlet velocity is taken as a true value for computing the error in average velocity computational methods. Comparison of average velocity computational methods is given in Table 5.3

Table 5.3 Comparison of averaging methods in geometry -4

Averaging Method	Computation Method	Average velocity, m/s	% error
Reduce point Averaging methods	1 point at (0.6 * d)	0.544638	8.927706
	1 point at (0.625 *d)	0.541632	8.326579
	2 points	0.517499	3.499885
	3 points	0.528903	5.780631
	3 points weighted	0.532881	6.576240
	4 points	0.534118	6.823763
	5 points	0.518471	3.694367
	6 points	0.523068	4.613738
Integration method (CSI)	4 Level integration	0.510143	2.028681
	5 Level integration	0.509715	1.943122
	6 Level integration	0.500201	0.040224
	8 Level integration	0.499599	-0.08012
Integration method (Power law Extrapolation & CSI)	4 Level power law	0.521385	4.277050
	5 Level power law	0.514802	2.960588
	6 Level power law	0.503277	0.655492
	8 Level power law	0.501817	0.363481

5.3.3 Results and Discussion

The velocity distribution in curved trapezoidal open channel is different from straight trapezoidal channel. 3D and 2D velocity contour of measurement section is created from measured data as shown in Fig 5.10. It is found that maximum velocity lies in upper right corner of measurement section.

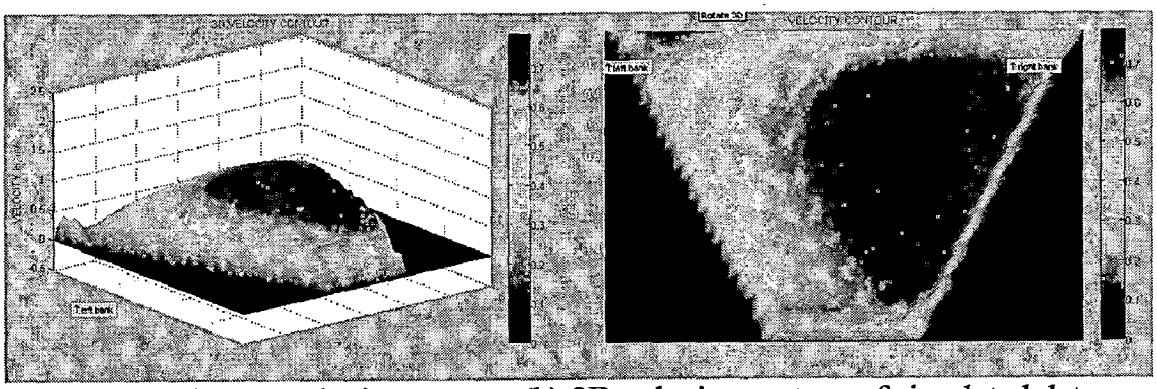

Fig 5.10 (a) 3D velocity contour (b) 2D velocity contour of simulated data

i. Two and Five points averaging method is accurate as compare to other averaging method.

ii. One-point method is give large error; therefore, it should not be used for computing the average velocity in the trapezoidal channel with 90° bend.

iii. As shown in Fig 5.11, CSI integration method is accurate as compare to power law extrapolation

iv. Average velocity is also computed by average width and power law extrapolation method from simulated data, its result is given in Table 5.4

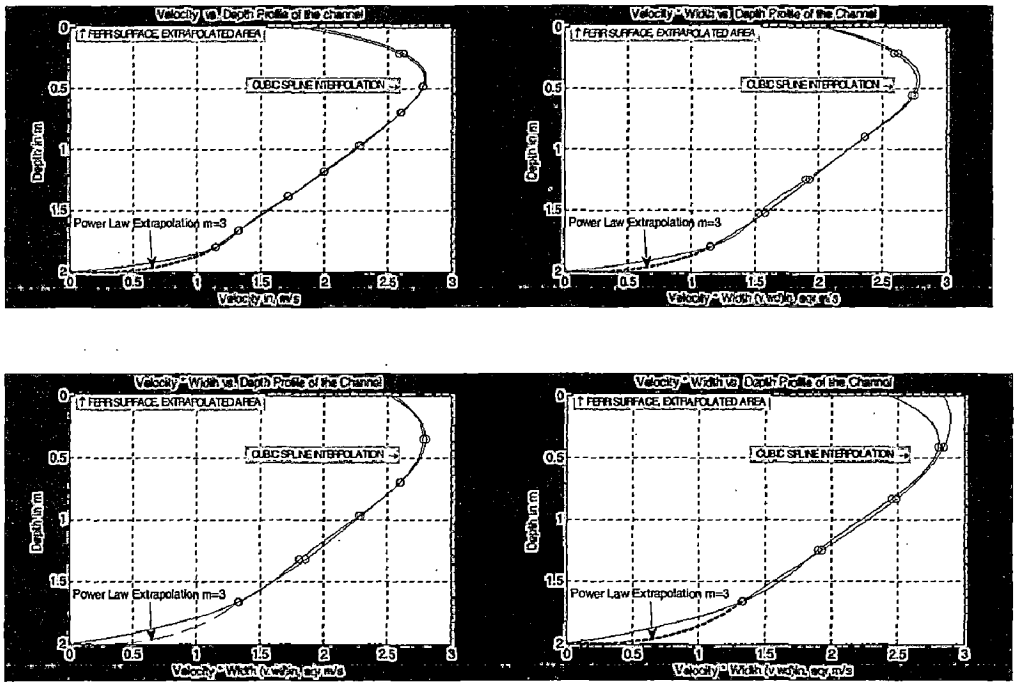

Fig 5.11 Comparison of vertical profiles of (a) 8 levels (b) 6 levels (c) 5 levels (d) 4 levels integration methods

Table 5.4 Comparison of integration method with m=3, 5 and 6(geometry -4)

Method	Average Velocity, m/s	% error
True value	0.5	--
Average width method	0.510934	2.18687
Integration method (Power law Extrapolation & CSI) with m=3	0.502086	0.41735
Integration method (Power law Extrapolation & CSI) with m=5	0.502651	0.50392
Integration method (Power law Extrapolation & CSI) with m=6	0.502988	0.59885

5.4 Trapezoidal Channel with Convergence (Geometry –5)

Convergence in the channel is also one of the major factors, which affect the velocity profile. Here the variation in the velocity profile caused due to a convergence is

studied by modeling the geometry and simulating the flow. An OUTLET plane is selected as the measuring section and velocity profile developed in the measuring section is analyzed. Geometry is meshed in GAMBIT as shown in Fig 5.12.

Channel dimension:

Depth=2m, Length= 35m, Angle=20.05°, Slope=0.00022 m / 1m, Side slope=2m /2m,

(Before convergence)Width at Bottom=5m, Width at Surface=8 m,

(After convergence) Width at Bottom= 2m, Width at Surface=6m,

Convergence length= 4m,

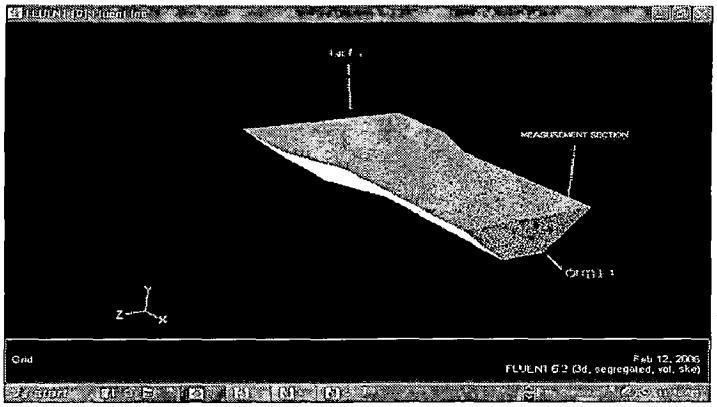

Fig 5.12 Trapezoidal channel with convergence

5.4.1 Profile Simulation in CFD

The convergence criteria are defined same as given in simple straight trapezoidal channel. Inlet boundary is initialized by 0.4 m/s. 200 iterations where given inside which the solution has converged. The simulation result of the flow in the channel is shown in Fig. 5.13. The velocity vs. width and partial discharge vs. depth profile is created from simulated matrix of data as shown in Fig 5.14.

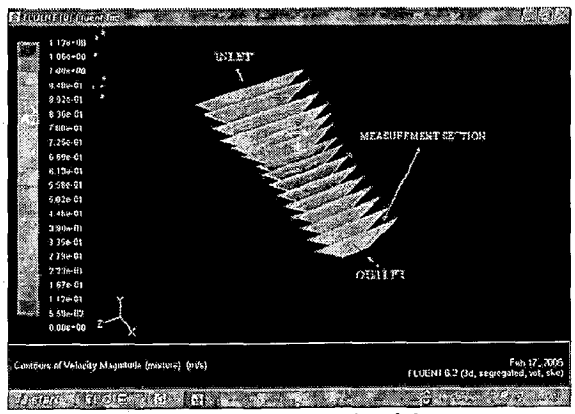

Fig 5.13 Velocity contour in a trapezoidal channel with convergence (Simulated in CFD)

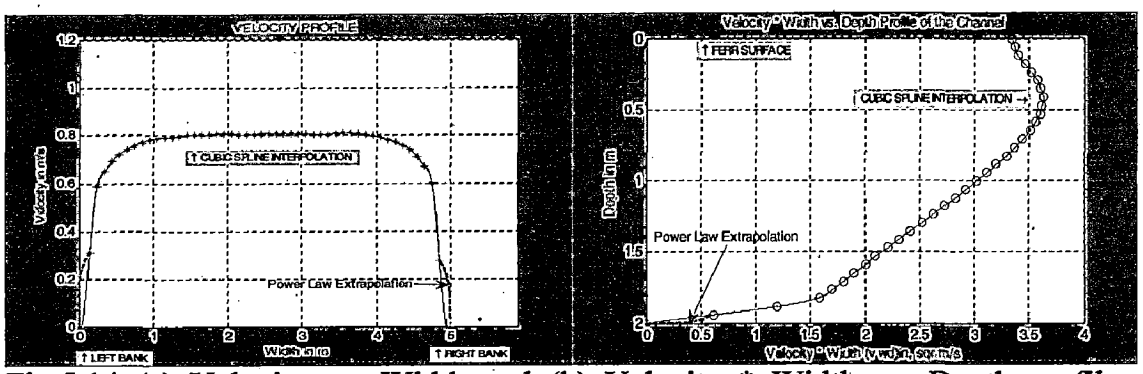

Fig.5.14 (a) Velocity vs. Width and (b) Velocity * Width vs. Depth profile of simulated data

5.4.2 Comparison of Average Velocity Computation Methods

In this case, true velocity at measurement section is calculated from known inlet discharge and known area of measurement section at outlet. Comparison of average velocity computational methods is given in Table 5.5

Table 5.5 Comparison of averaging methods in geometry -5

Averaging Method	Computation Methods	Average velocity, m/s	% error
Reduce point Averaging methods	1 point at (0.6 * d)	0.769072	9.876742
	1 point (0.625 *d)	0.768879	9.839857
	2 points	0.726383	3.769000
	3 points	0.740612	5.801714
	3 points weighted	0.747727	6.818142
	4 points	0.744747	6.392428
	5 points	0.727344	3.906285
	6 points	0.733786	4.826571
Integration method (CSI)	4 Level integration	0.679655	-2.906290
	5 Level integration	0.693132	-0.981080
	6 Level integration	0.699418	-0.08302
	8 Level integration	0.698790	-0.172775
Integration method (Power law Extrapolation & CSI)	4 Level power law	0.714671	2.095867
	5 Level power law	0.711271	1.610282
	6 Level power law	0.700659	0.094252
	8 Level power law	0.701376	0.196623

5.4.3 Results and Discussion

3D and 2D velocity contour of measurement section is created from simulated data as shown in Fig 5.15. The velocity magnitude in trapezoidal open channel with convergence is increased after convergence and velocity is uniformly distributed with maximum in middle section of channel.

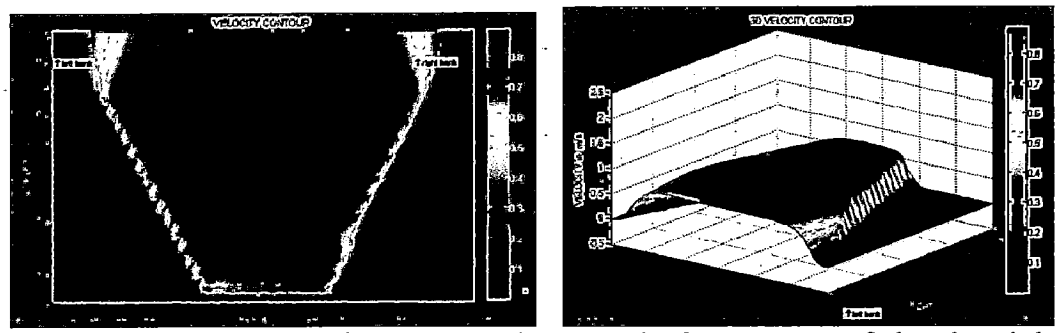

Fig 5.15 (a) 3D velocity contour (b) 2D velocity contour of simulated data

i. Two point averaging method is good as compare to other reduce point averaging methods.

ii. Accuracy of integration method is increased, as number of partial discharge data increase.

iii. Result of average width method and integration method with different value of power law exponent as given in Table 5.6.

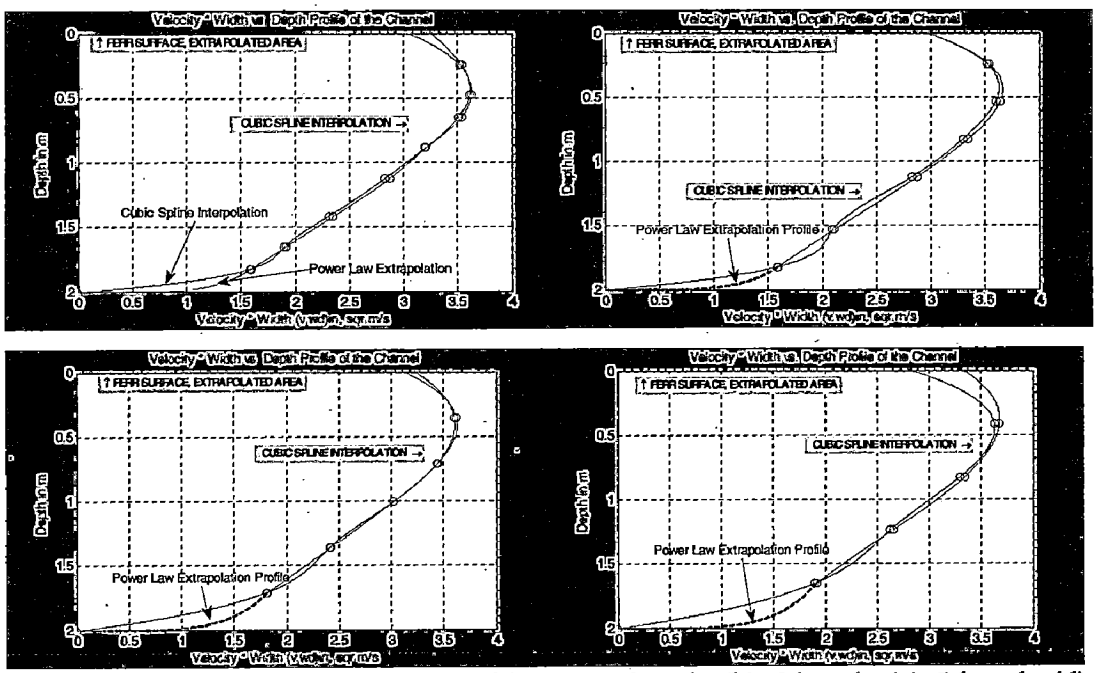

Fig 5.16 Comparison of vertical profiles (a) 8 levels (b) 6 levels (c) 5 levels (d) 4 levels integration methods

Table 5.6 Comparison of integration method with m=3, 5 and 6(geometry -5)

Method	Average Velocity, m/s	% error
True value	0.7	---
Average width method	0.710562	1.508962
Integration method (Power law Extrapolation & CSI) with m=3	0.705256	0.750941
Integration method (Power law Extrapolation & CSI) with m=5	0.706192	0.884581
Integration method (Power law Extrapolation & CSI) with m=6	0.706827	0.975324

5.5 Straight Semi-Trapezoidal Channel (Geometry –6)

In this section, the velocity profile in a semi-trapezoidal geometry is studied by modeling the geometry and simulating the flow. Geometry is meshed in GAMBIT as shown in Fig 5.17

Channel dimension

Depth – 2m, Length – 30m, Width at Bottom– 4m, Width at Surface=6,

Slope = 0.00022 m / 1m, Side slope- 2m /2m

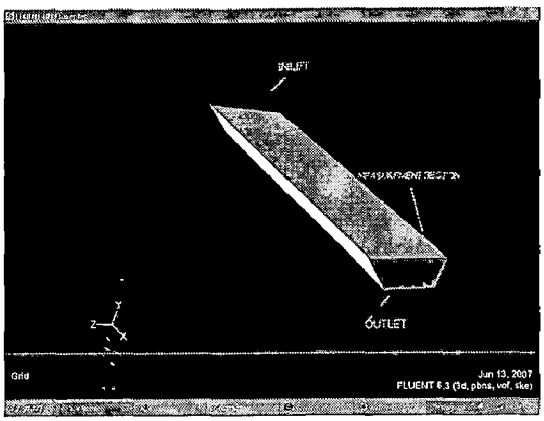

Fig. 5.17 Straight semi-trapezoidal open channel

5.5.1 Profile Simulation in CFD

The convergence criteria are defined same as given in simple straight trapezoidal channel. Except the average velocity magnitude in inlet, this is given as 0.4 m/s. After the parameters are set, the solver is initialized with inlet conditions and the iteration is done. 200 iterations where given inside which the solution has converged. The simulation result

of the flow in the channel is shown in Fig 5.18. The velocity vs. width and partial discharge vs. depth profile is created from simulated matrix of data as shown in Fig 5.19. It is observed the low velocity at upper corner of trapezoidal section.

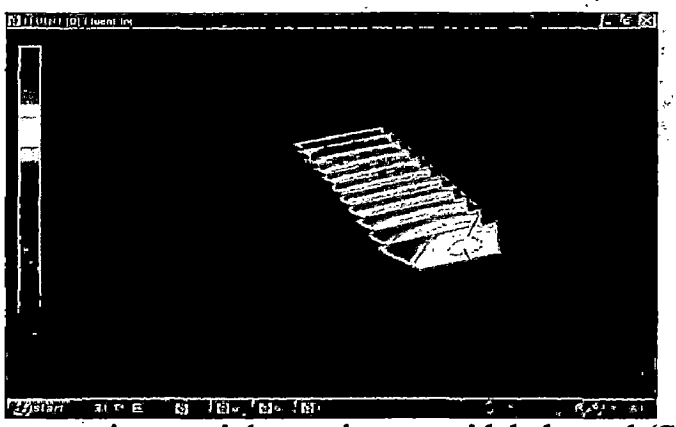

Fig 5.18 Velocity contour in a straight semi-trapezoidal channel (Simulated in CFD)

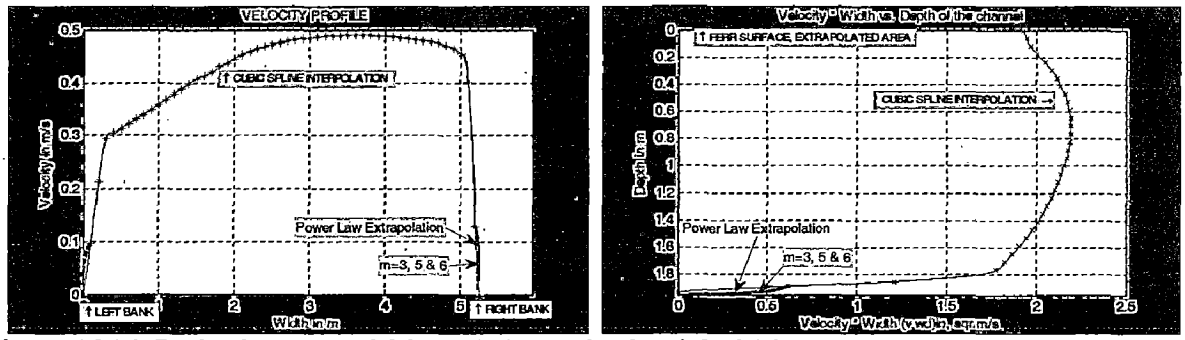

Fig. 5.19(a) Velocity vs. Width and (b) Velocity * Width vs. Depth profile of simulated data

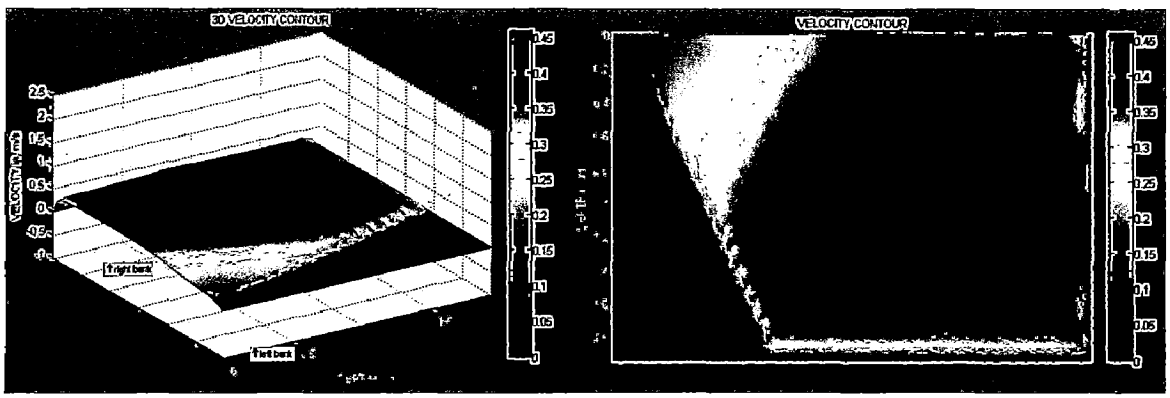

Fig 5.20 (a) 3D velocity contour (b) 2D velocity contour of simulated data

5.5.2 Comparison of Average Velocity Computation Methods

Inlet velocity is taken as a true value for computing the error in average velocity computational methods. Comparison of average velocity computational methods is given in Table 5.7

Table 5.7 Comparison of averaging methods in geometry -6

Averaging Method	Computation Method	Average velocity, m/s	% error
Reduce point Averaging methods	1 point at (0.6 * d)	0.442436	10.60904
	1 point (0.625 *d)	0.443726	10.93168
	2 points	0.413291	3.322939
	3 points	0.422970	5.742677
	3 points weighted	0.427810	6.952550
	4 points	0.424583	6.145970
	5 points	0.414904	3.726229
	6 points	0.417378	4.344607
Integration method (CSI)	4 Level integration	0.389029	-2.74259
	5 Level integration	0.392600	-1.84398
	6 Level integration	0.396201	-0.94965
	8 Level integration	0.399406	-0.14834
Integration method (Power law Extrapolation & CSI)	4 Level power law	0.415791	3.394788
	5 Level power law	0.410887	2.721984
	6 Level power law	0.400681	0.170473
	8 Level power law	0.401162	0.290596

5.5.3 Results and Discussion

The velocity distribution in a straight semi-trapezoidal open channel is different from the trapezoidal channel. 3D and 2D velocity contour of measurement section is created from measured data as shown in Fig 5.20.

i. Maximum velocity is distributed at rectangular section of semi trapezoidal channel.
ii. Three-point method is accurate as compare to three point weighted method.
iii. Accuracy of integration method may be increase by choosing small value of power law exponent m.

Table 5.8 Comparison of integration method with m=3, 5 and 6(geometry -6)

Method	Average Velocity, m/s	% error
True value	0.4	----
Integration method (Power law Extrapolation & CSI) with m=3	0.402614496	0.6536241
Integration method (Power law Extrapolation & CSI) with m=5	0.403139009	0.7847523
Integration method (Power law Extrapolation & CSI) with m=6	0.403413524	0.8533851

5.6 Semi-Trapezoidal Channel with Convergence (Geometry-7)

Convergence in the channel is one of the major factors, which affect the velocity profile. Here the variation in the velocity profile caused due to a convergence is studied by modeling the geometry and simulating the flow. Geometry is meshed in GAMBIT as shown in Fig 5.21

Channel dimension

Depth= 2m, Length= 30m, Angle=14.04°, Slope=0.00022 m / 1m, Side slope=2m /2m

(Before convergence)--Width at Bottom= 4m, Width at Surface=6 m,

(After convergence) --Width at Bottom= 2m, Width at Surface=4m,

Convergence length=4m,

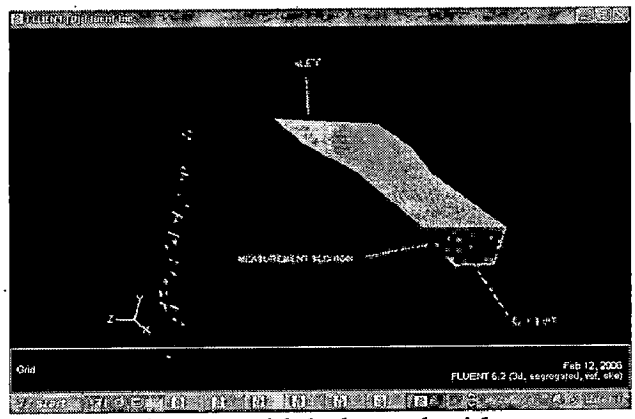

Fig.5.21 Semi-trapezoidal channel with convergence

5.6.1 Profile Simulation in CFD

The inlet boundary is initialized by 0.3 m/s average velocity. The velocity contour profile of simulated channel is shown in Fig.5.22. The velocity vs. width and partial

discharge vs. depth profile is created from simulated matrix of data, and maximum velocity is found in middle of channel as shown in Fig 5.23.

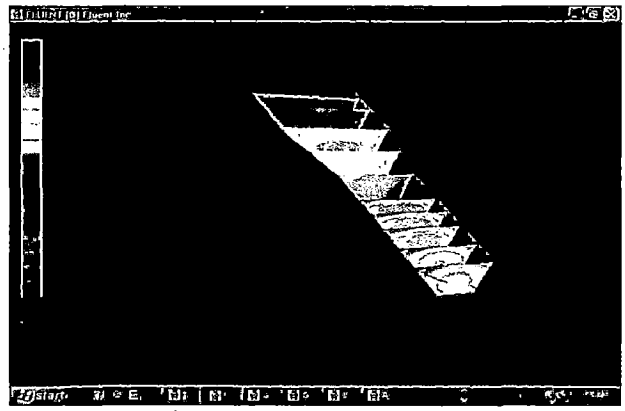

Fig 5.22 Velocity contour in a semi-trapezoidal channel with convergence

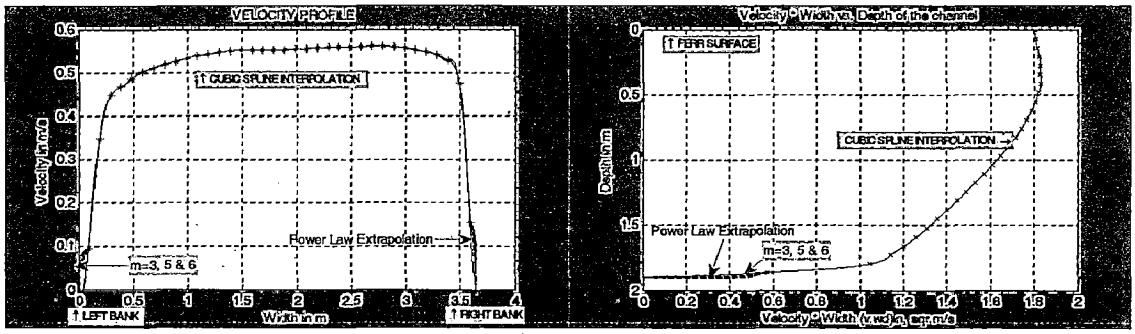

Fig.5.23 (a) Velocity vs. Width and (b) Velocity * Width vs. Depth profile of simulated data

5.6.2 Comparison of Average Velocity Computation Methods

In this case, true velocity at measurement section is calculated from known inlet discharge and known area of measurement section at outlet. Comparison of average velocity computation methods is given in Table 5.9

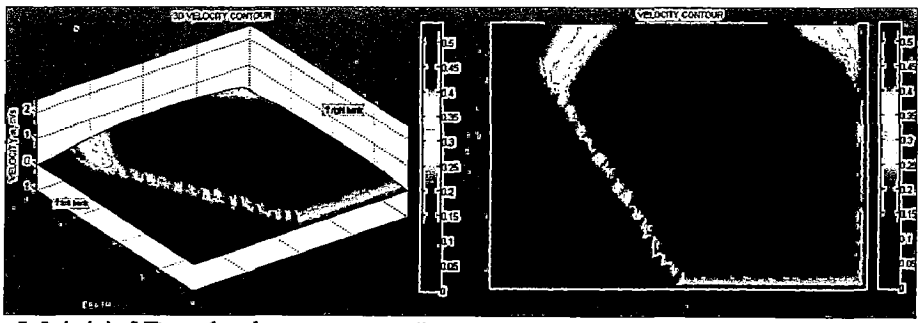

Fig 5.24 (a) 3D velocity contour (b) 2D velocity contour of simulated data

Table 5.9 Comparison of averaging methods in geometry -7

Averaging Method	Computation Method	Average velocity, m/s	% error
Reduce point Averaging methods	1 point at (0.6 * d)	0.541877	8.375568
	1 point (0.625 *d)	0.538952	7.790484
	2 points	0.514423	2.884780
	3 points	0.523537	4.707541
	3 points weighted	0.528150	5.630174
	4 points	0.526125	5.225116
	5 points	0.514536	2.907283
	6 points	0.518568	3.717399
Integration method (CSI)	4 Level integration	0.492169	-1.566141
	5 Level integration	0.493554	-1.289194
	6 Level integration	0.506907	1.381442
	8 Level integration	0.503538	0.707603
Integration method (Power law Extrapolation & CSI)	4 Level power law	0.496503	-0.699255
	5 Level power law	0.498563	-0.328725
	6 Level power law	0.502814	0.562990
	8 Level power law	0.502295	0.459155

5.6.3 Results and Discussion

The velocity distribution in semi-trapezoidal open channel with convergence is different from the trapezoidal open channel with convergence. Maximum velocity is found in middle section and it gradually decrease toward surrounding boundary. 3D and 2D velocity contour of measurement section is created from measured data as shown in Fig 5.24

i. Integration method by power law extrapolation and cubic spline interpolation is accurate as compare to integration method by CSI.

ii. Average velocity from simulated data is computed by integration method with different value of power law exponent as given in Table 5.10.

Table 5.10 Comparison of integration method with m=3, 5 and 6(geometry -7)

Method	Average Velocity m/s	% error
True value	0.5	---
Integration method (Power law Extrapolation & CSI) with m=3	0.502728	0.545778
Integration method (Power law Extrapolation & CSI) with m=5	0.503962	0.792590
Integration method (Power law Extrapolation & CSI) with m=6	0.504038	0.807738

5.7 Semi-Trapezoidal Channel with Divergence (Geometry 8)

Here the variation in the velocity profile caused due to a divergence is studied by modeling the geometry and simulating the flow. Maximum velocity immediately after divergence is found at middle of the channel and it uniformly distributed at 10 or 15 meter away after divergence. An OUTLET plane is selected as the measuring section and velocity profile developed in the measuring section is analyzed. Geometry is meshed in GAMBIT as shown in Fig 5.25

Channel dimension

Depth=2m, Length=30m, Angle=14.04°, Slope=0.00022 m / 1m, Side slope= 2m /2m

(Before convergence)--Width at Bottom=3m, Width at Surface=5 m,

(After convergence) --Width at Bottom=5m, Width at Surface=7m,

Divergence length=4m,

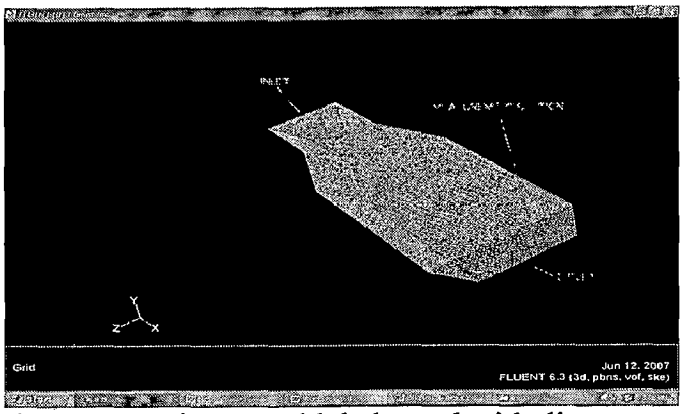

Fig 5.25 Semi-trapezoidal channel with divergence

5.7.1 Profile Simulation in CFD

The inlet boundary is initialized by 0.75 m/s average velocity. The velocity contour profile of simulated channel is shown in Fig.5.26. It is observed the maximum velocity in middle section after the convergence. The velocity vs. width and partial discharge vs. depth profile is created from simulated matrix of data as shown in Fig 5.27. It is observed in horizontal profile that power law extrapolation with m=six is not following smooth profile.

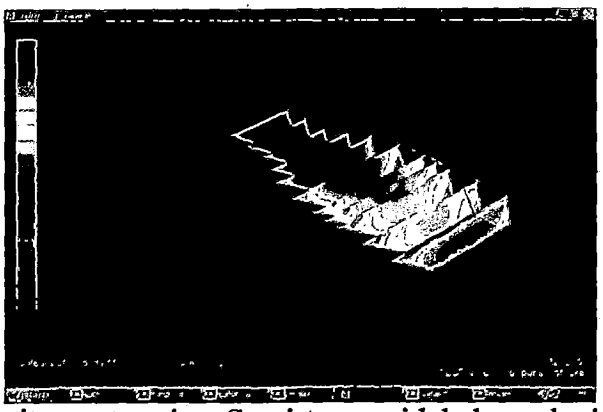

Fig 5.26 Velocity contour in a Semi-trapezoidal channel with divergence

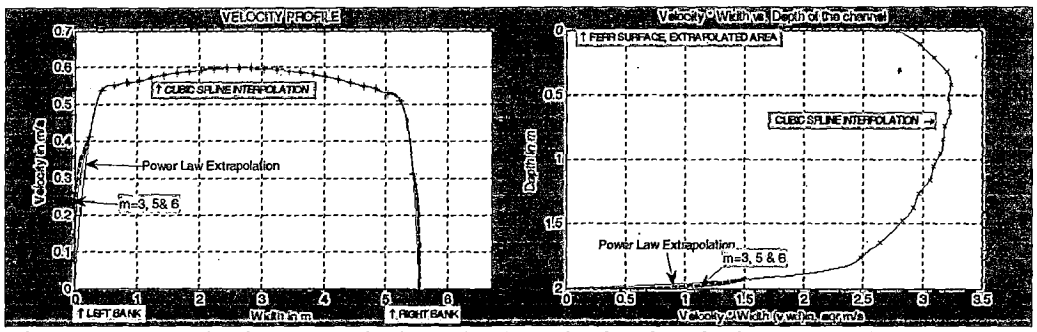

Fig 5.27 (a) Velocity vs. Width and (b) Velocity * Width vs. Depth profile of simulated data

5.7.2 Comparison of Average Velocity Computation Methods

Velocity magnitude at inlet is more than velocity at outlet. Therefore, true velocity at outlet is determined from known discharge. True velocity at outlet is used for analyzing the error uncertainty in average velocity computation methods. Comparison of average velocity computational methods is given in Table 5.11.

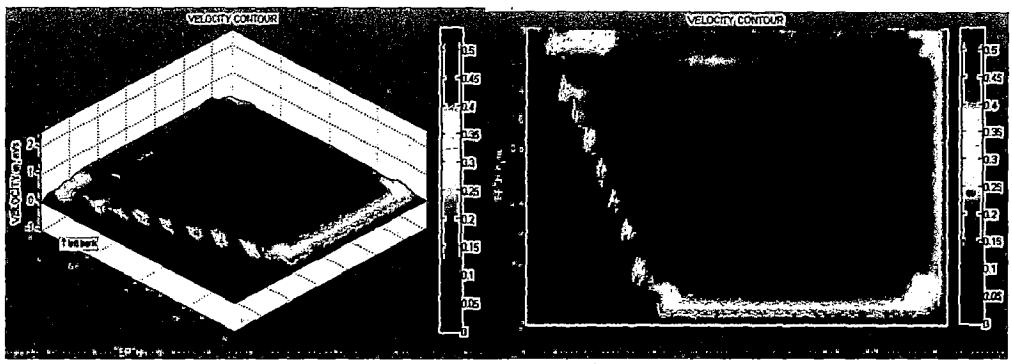

Fig 5.28 (a) 3D velocity contour (b) 2D velocity contour of simulated data

Table 5.11 Comparison of averaging methods in geometry -8

Averaging Method	Computation Method	Average velocity, m/s	% error
Reduce point Averaging methods	1 point at (0.6 * d)	0.550939	10.187934
	1 point (0.625 *d)	0.548242	9.648567
	2 points	0.518240	3.641232
	3 points	0.535882	7.176470
	3 points weighted	0.539590	7.918102
	4 points	0.536444	7.288842
	5 points	0.521386	4.277383
	6 points	0.522847	4.569539
Integration method (CSI)	4 Level integration	0.492262	-1.547592
	5 Level integration	0.490306	-1.93864
	6 Level integration	0.504835	0.967086
	8 Level integration	0.502697	0.539509
Integration method (Power law Extrapolation & CSI)	4 Level power law	0.510445	2.089194
	5 Level power law	0.508173	1.634741
	6 Level power law	0.503543	0.70874
	8 Level power law	0.502015	0.403170

5.7.3 Results and Discussion

The velocity is uniformly distributed in semi-trapezoidal open channel with divergence at measurement section. 3D and 2D velocity contour of measurement section is created from measured data as shown in Fig 5.28

i. Six and eight level integration method is accurate as compare to other methods.

ii. Average velocity from simulated data is computed by integration method with different value of power law exponent as given in Table 5.12.

Table 5.12 Comparison of integration method with m=3, 5 and 6(geometry -8)

Method	Average Velocity m/s	% error
True value	0.5	0
Integration method (Power law Extrapolation & CSI) with m=3	0.503224	0.644868
Integration method (Power law Extrapolation & CSI) with m=5	0.503926	0.785352
Integration method (Power law Extrapolation & CSI) with m=6	0.504264	0.853292

5.8 Overall Comparison

In this work, eight geometries are simulated by CFD analysis. Reduce point averaging methods and integration methods are used for computing the average velocity in various open channel geometries. Error in average velocity computation is calculated with reference to inlet velocity condition defined in geometry simulation in CFD.

Comparison of averaging methods is shown in Fig 5.29. X-axis is geometry number that is given in chapter 4 & 5. Y-axis is percentage error in average velocity computation by various average velocity computational methods in all open channels geometry. Number is given to average velocity computation method according to sequence given in comparison table of averaging methods in simulation section.

Comparison of error in reduce point averaging methods is shown in Fig 5.29. It is observed the two point and five point methods are accurate as compared to other reduce point averaging methods.

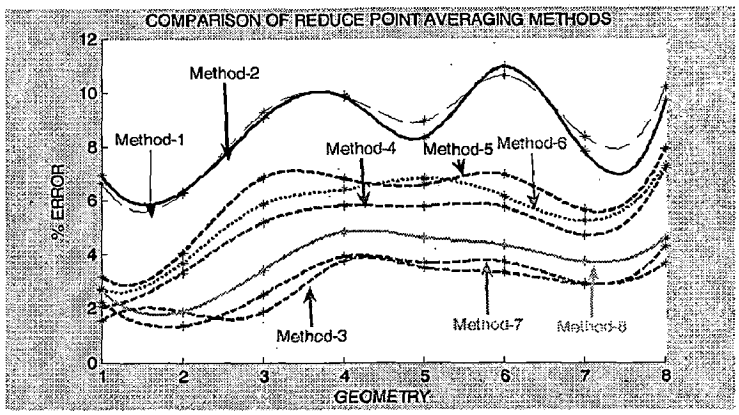

Fig 5.29 Comparison of reduce point averaging methods

Average velocity in trapezoidal open channels has been computed by integration method using cubic spline interpolation (CSI). Comparison of error in average velocity computation by integration method is shown in Fig 5.30. It is observed the six and eight levels integration methods are accurate as compared to four and five levels integration methods.

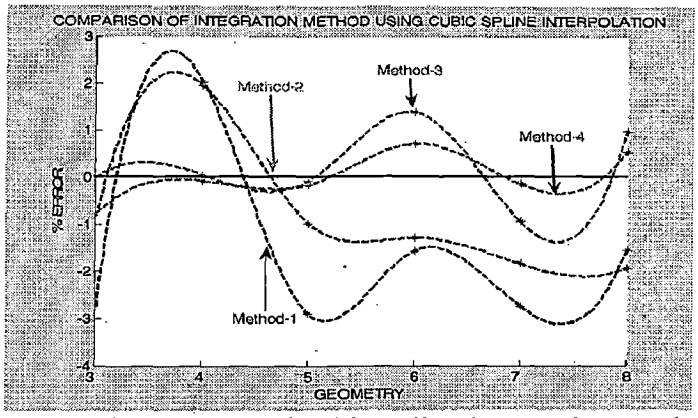

Fig 5.30 Comparison of cubic spline integration method

Average velocity in six different geometries is computed by integration method using CSI and power law extrapolation. Error in average velocity computation has been calculated in simulation section. As shown in Fig 5.31, six and eight levels integration method using power law extrapolation and CSI are accurate as compared to five and four levels integration method.

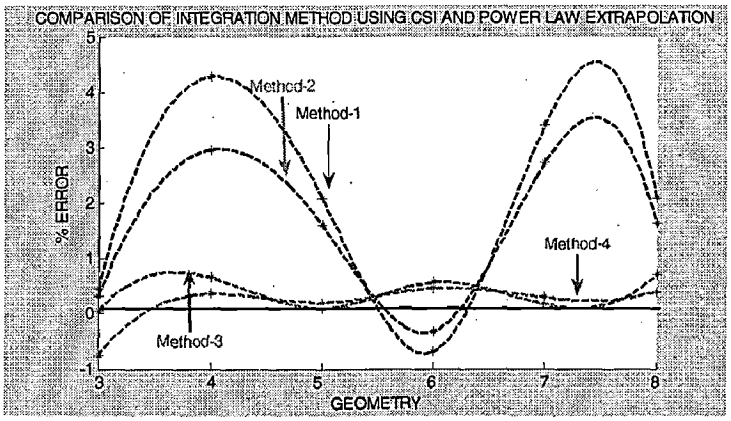

Fig 5.31 Comparison of integration method using CSI and power law

Six and eight levels integration method using Power law extrapolation and CSI are accurate as compared to other average velocity computational methods.

One point method is not good option for open channel average velocity measurement.

CHAPTER 6
CONCLUSION

6.1 Summary

From comparison of H-ADCP and PCM, it is observed the non-intrusiveness of H-ADCP can yield better accuracy as compared to intrusive of PCM. Accurate discharge measurement with PCM requires the precise placement and number as proposed by IEC-60041 and ISO-748. Likewise, accuracy of placement of H-ADCP significantly influences accuracy of measurement.

Six trapezoidal channels and two rectangular open channels have been simulated by CFD analysis. Average velocity from simulated data is computed by using averaging and integration methods. It is observed that the two point averaging method is a good option for average velocity computation in trapezoidal open channels as compared to one point method. Accuracy of integration method can be increased by increasing the number of measurement horizontal section. Average width method should not be used for trapezoidal channel with large width of trapezoidal section. Two rectangular channels have been simulated and it is observed the maximum velocity in narrow channel lies below free surface and in wide channel near the free surface.

6.2 Future Scope

Scope of research as an extension to the work done here is very wide. A few suggestions are given below:

(i) CFD analysis of six trapezoidal geometries is done in this work. The work can be extended to develop and analyze the profiles for various other geometries of open channel.

(ii) In this work, Accuracy of H-ADCP is compared with PCM. This work can be extended to reliability testing of H-ADCP by comparing with theoretical data.

(iii) Accuracy of average velocity computation methods is analyzed here, this work can be extend to analyze the effect of averaging and sampling time on accuracy of average velocity measurement in open channel.

(iv) Error in integration method by using power law extrapolation and cubic spline interpolation scheme is analyzed here. As measured data reduces, the velocity data cannot be accurately interpolated by cubic spline interpolation. Integration method by using another curve-fitting scheme such as support vector machine (SVM) and artificial neural network can be taken as a further advancement in this work.

REFERENCES

[1] Fluent User Services Centre, "Introduction to CFD Analysis, Introductory Fluent Notes", 2002.

[2] Herschy R W, "The Uncertainty in a Current Meter Measurement", Elsevier-Flow Measurement and Instrumentation, Vol.13, 2002, pp. 281–284.

[3] ISO-1088, "Liquid Flow Measurement in Open Channels Velocity Area Methods-Collection and Processing of Data for Determination of Errors in Measurement", Second edition, 1985.

[4] Simpson Michael R, "Discharge Measurement Using a Broad-band Acoustic Doppler Current Profiler", US Geological survey, Sacramento, California 2001.

[5] WinH-ADCP Users Guide, RD Instruments, 2005.

[6] ISO-748, "Measurement of Liquid Flow in Open Channels - Velocity-Area Methods", Third edition, 1997.

[7] Fenton John D, "The Application of Numerical Methods and Mathematics to Hydrography", Australian Hydrographic Conference, Sydney, 2002.

[8] IEC-60041, "Field acceptance tests to determine the hydraulic performance of hydraulic turbines, storage pumps and pump turbines", 1991.

[9] Gonzalez-Castro Juan A, Kevin A, and Duncker James J, "Effect of temporal Resolution on the Accuracy of ADCP Measurements", Water Resources engineering and water resources planning & management conference USA, 2000.

[10] Wang F and Huang H, "Horizontal Acoustic Doppler current profiler (H-ADCP) for Real Time Open Channel Flow Measurement: Flow Calculation Model and Field Validation", Submitted to 31st IAHR Congress 2005.

[11] Must M, Yu K, and SpasoJevic M," Practical Aspects of ADCP data use for Quantification of Mean River Flow Characteristics; Part I: Moving-Vessel Measurements", Science Direct-Flow Measurement and Instrumentation, Vol.15, 2004, pp. 1-16.

[12] Must M, Yu K, Pratt T, and Abraham D," Practical Aspects of ADCP data use for Quantification of Mean River Flow Characteristics; Part II: Fixed-Vessel

Measurements", Science Direct-Flow Measurement and Instrumentation, Vol.15, 2004, pp. 17-28.

[13] Franca M J and Lemmin U, "Eliminating Velocity Aliasing in Acoustic Doppler Velocity profiler data", Institute of Physics Publishing, 2006.

[14] Doering J C and Hans P D, "Turbine Discharge Measurement by the Velocity-Area Method", Journal of Hydraulic Engineering, Vol. 127, No. 9, 2001.

[15] Taylor Randolph J., "Interpolation Using the Cubic Spline Function", Pi Mu Epsilon Journal, Vol. 6, No. 7, pp. 387-393.

[16] Simpson M R and Bland R, "Methods for Accurate Estimation of Net Discharge in a Tidal Channel", IEEE Journal of Oceanic Engineering, Vol.25, No 4, 2000.

[17] Versteeg H K and Malalasekera W, "An introduction to CFD- The finite volume method", Longman Group Ltd. 1995.

[18] Goring Derek G, Walsh Jeremy M., "Modeling the Distribution of Velocity in a River Cross-section", New Zealand Journal of Marine and Freshwater Research, Vol. 31, 1997, pp. 155-162.

[19] Gonzalez Juan A, Melching Charles S, and Oberg Kevin A, "Analysis of Open Channel Velocity Measurements Collected with an Acoustic Doppler Current Profiler", Proc. RiverTech, IWRA, Chicago, Illinois, Vol. 2, 1996, pp.838-845.

[20] Souders D T and Hirt C W, "Modeling Roughness Effects in Open Channels", Flow Science Inc. 2002

[21] Seo, Won II and Baek, K O, "Estimation of the Longitudinal Dispersion Coefficient Using the Velocity Profiles in Natural Streams", Journal of Hydraulic Engineering-Trans ASCE, Vol. 130, No. 3, 2004, pp. 227-236.

[22] Schlichting H, "Boundary Layer Theory", Seventh Edition, McGraw-Hill, New York, 1979.

[23] Sarma Kandula V N, Ramana Prasad B V and Sarma A K, "Detailed Study of Binary Law for Open Channels", Journal of Hydraulic Engineering, Vol. 126, No. 3, 2000.

[24] Chiu Chao-Lin, M ASCE, and Tung Ning-Chien, "Maximum Velocity And Regularities In Open-Channel Flow", Journal of Hydraulic Engineering, ASCE, Vol. 128, No. 4, 2001, pp. 390-398.